Catalysis Reviews: Science and Engineering
Publication details, including instructions for authors and subscription information:
http://www.tandfonline.com/loi/lctr20

The Acidity of Zeolites: Concepts, Measurements and Relation to Catalysis: A Review on Experimental and Theoretical Methods for the Study of Zeolite Acidity

E.G. Derouane [a b], J.C. Védrine [c], R. Ramos Pinto [a d], P.M. Borges [a], L. Costa [a], M.A.N.D.A. Lemos [a], F. Lemos [a] & F. Ramôa Ribeiro [a]

[a] IBB - Institute for Biotechnology and Bioengineering, Centre for Biological and Chemical Engineering, Instituto Superior Técnico, Universidade Técnica de Lisboa, Lisboa, Portugal

[b] Faculdade de Ciências e Tecnologia, Centro de Investigação em Química e Catálise, Universidade do Algarve, Faro, Portugal

[c] Laboratoire de Réactivité de Surface, Université P. & M. Curie, Paris, France

[d] ISCSP, Universidade Técnica de Lisboa, Pólo Universitário do Alto da Ajuda, Lisboa, Portugal

Published online: 13 Sep 2013.

To cite this article: E.G. Derouane, J.C. Védrine, R. Ramos Pinto, P.M. Borges, L. Costa, M.A.N.D.A. Lemos, F. Lemos & F. Ramôa Ribeiro (2013) The Acidity of Zeolites: Concepts, Measurements and Relation to Catalysis: A Review on Experimental and Theoretical Methods for the Study of Zeolite Acidity, Catalysis Reviews: Science and Engineering, 55:4, 454-515, DOI: 10.1080/01614940.2013.822266

To link to this article: http://dx.doi.org/10.1080/01614940.2013.822266

Catalysis Reviews: Science and Engineering, 55:454–515, 2013

ISSN: 0161-4940 print / 1520-5703 online
DOI: 10.1080/01614940.2013.822266

The Acidity of Zeolites: Concepts, Measurements and Relation to Catalysis: A Review on Experimental and Theoretical Methods for the Study of Zeolite Acidity

E.G. Derouane[1,2], J.C. Védrine[3], R. Ramos Pinto[1,4], P.M. Borges[1], L. Costa[1], M.A.N.D.A. Lemos[1], F. Lemos[1], and F. Ramôa Ribeiro[1]

[1]IBB – Institute for Biotechnology and Bioengineering, Centre for Biological and Chemical Engineering, Instituto Superior Técnico, Universidade Técnica de Lisboa, Lisboa, Portugal
[2]Faculdade de Ciências e Tecnologia, Centro de Investigação em Química e Catálise, Universidade do Algarve, Faro, Portugal
[3]Laboratoire de Réactivité de Surface, Université P. & M. Curie, Paris, France
[4]ISCSP, Universidade Técnica de Lisboa, Pólo Universitário do Alto da Ajuda, Lisboa, Portugal

In this article, we considered all aspects of acidity (nature of acid sites, strength, density, etc.) in solid catalysts and in zeolites in particular. After reminding the definition of acidity in liquid and solid acids, we emphasized acidity characterization by the most used physical techniques, such as Hammett's indicator titration, microcalorimetry of adsorbed probe molecules (ammonia, pyridine or other amines for acidity characterization and CO_2 or SO_2 for basicity characterization), ammonia or any amine thermodesorption, IR spectroscopy of hydroxyl groups and of several probe molecules adsorbed (ammonia, pyridine, piperidine, amines, CO, H_2, etc.), MAS-NMR of ^{27}Al, ^{29}Si, ^{1}H elements and of ^{1}H, ^{13}C, ^{31}P, etc. of adsorbed probe molecules, and model catalytic reactions.

Modeling the way the acid features of zeolites influence the catalytic activity of these catalysts toward acid-catalyzed reactions (relation between ammonia desorption

Received December 21, 2012; accepted June 12, 2013.

Address correspondence to J.C. Védrine, Laboratoire de Réactivité de Surface, Université P. & M. Curie, 4 place Jussieu, F-75252 Paris, France. E-mail: jacques.vedrine@upmc.fr

activation energy values and catalytic activities, reaction mechanism, and kinetics) completes the general analysis of acidity and zeolite chemistry.

Keywords Acidity, Zeolites, Acidity characterization, Model reactions, Acidity-activity relationships

1. INTRODUCTION

The concept of solid acids is of major importance in many aspects related to the applications of solid surfaces and, in particular, for catalytic purposes. Acid catalysis is one of the most important areas of catalysis, both homogeneous and heterogeneous, with countless applications in our world and in the chemical industry.

Although the concepts related to homogeneous acids are well understood and even grasped by the general public, the concepts associated with the acidity of solids are somewhat more elaborate. The original concept of the acid strength of solids was developed by Walling in the 1950s to characterize the ". . . ability (of a surface) to convert an adsorbed neutral base to its conjugate acid" (1). Walling suggested that the surface acid strength could be quantified by using the Hammett acidity function, H_0, with the indicator method developed earlier for solutions (2). The characterization and probing of the surface acidity of solids has evolved much since then and remains an open subject of definite importance (3).

In the Brønsted theory, an acid is defined as a *proton donor* and a base as a *proton acceptor* (a base must have a pair of electrons available to share with the proton). An acid-base reaction is a transfer of a proton from an acid to a base. The new species formed is then a base referred to as *conjugate base* of the acid. They fit the equation below, where the upper bar represents an electron doublet:

$$\mathrm{A-H} + \overline{B}^{-} \leftrightarrows \overline{A}^{-} + \mathrm{B-H}$$

$$\mathrm{Acid} + \mathrm{Base} \leftrightarrows \mathrm{Base} + \mathrm{Acid}.$$

An acid has one positive charge higher than its conjugate base. The classification of acid catalyzed reactions has been usually associated with homogeneous acid catalysis. It is usually accepted that reactions may be catalyzed by acid or base in two different ways, called *general* and *specific* catalyses. If the rate of an acid reaction in a solvent S is proportional to $[SH^+)$, the reaction is said *specific*, the acid being SH^+, the rate being derived from $S + HA \Delta SH^+ + A^-$, while the acid HA introduced in the solvent can be stronger or weaker than SH^+. In water, SH^+ is H_3O^+. In *general* acid catalysis, the rate increases with $[SH^+)$ but also with the concentration of other acids HA. Thus,

specific acid catalysis occurs when the main catalytic species is the acid form of the solvent, i.e., when it is the solvent which is responsible for transferring the proton to the reactants so that they can proceed to the products, while *general* acid catalysis occurs when any acid species present in the reaction medium may intervene in the catalytic process.

The ability of a certain species to accelerate a reaction by acid catalysis depends, of course, on the acid strength (the tendency of the acid species to transfer a proton to another species) of that species. The relationship between the acid strength of a catalyst and its catalytic ability towards a certain reaction can, for instance, be expressed by the Brønsted equation

$$\log k = \alpha \log K_a + C$$

with k being the rate constant for the reaction catalyzed by a given acid, K_a the ionisation constant of that acid and C is a constant that can be interpreted as the logarithm of the reaction rate constant for an acid with a unit ionization constant. If one considers the reaction to be carried out in water and, thus, K_a corresponds to the ionization constant of the acid in water, C would be the reaction rate constant when catalyzed by water.

The reason for this type of relation lies on the fact that the mechanism of an acid-catalyzed reaction always involves the transfer of a proton from the acid species that acts as catalyst to one of the reactants. In fact, for an acid-catalyzed reaction, one may write:

$$\text{Step1}: \qquad A + SH^+ \leftrightarrows AH^+ + S$$

$$\text{Step2}: \qquad AH^+ \rightarrow \text{products}$$

and, thus, the catalytic activity depends on the concentration of AH^+, which increases as the acidity of SH^+ increases.

At about the same time that Brønsted proposed his acid-base theory, Lewis put forth a broader theory in which an acid is any species with a vacant orbital that can accept a pair of electrons, while a base is a species that has an unshared pair of electrons. In the acid-base reaction, the unshared electron pair of the base forms a covalent bond with the vacant orbital of the acid, according to the equation:

$$A + \overline{B} \rightarrow A - B.$$

In Brønsted's view, an acid is a proton donor, while in Lewis's view, the acid is an electron acceptor; according to this view, a Brønsted acid is not a Lewis acid, although the proton itself is an acid, as it has a vacant orbital that bonds to the base and, by doing so, releases a basic species. A Lewis base, however,

is also a Brønsted base, since it is always capable of donating its unshared electron pair to a proton.

At this point it should be noted that the acid strength of a given acidic species is usually measured in a relative scale, as the measure is usually a thermodynamic constant that quantifies the relative acidity of the species under consideration with a "standard" or "reference" base.

For instance, the acid strength for acids in aqueous medium is usually measured by the dissociation constant of the acid in water, i.e., a measurement of the relative acidity of the species when compared to water.

The same principles apply to acids on solid surfaces. For all practical purposes, the model of Walling treated a solid acidic surface as a proton-donating medium with a catalytic activity determined only by the concentration of universal "acid" protons, H^+. Thus, the acid strength of the surface acid sites can be measured by the ionization constant or, for a more convenient scale, by $pK_a = -\log_{10} K_a$.

Since the acidity is measured using a reference base, Hammett constructed a visual acidity scale by resorting to colored indicators. He defined the H_0 acidity function as $H_0 = -\log(h_0)$, with $h_0 = a_{H+} \cdot f_I / f_{HI+}$ where a_{H+} is the activity of the proton and f_I and f_{HI+} the activity coefficients of the colored indicator, which are used to build the acidity scale, and of its conjugate acid. Such colored indicators are weak bases (B) that can easily be converted to the corresponding conjugate acid BH^+ by stronger acids.

The titration of acid sites with bases and indicators was introduced by Benesi (4,5), Hirschler and Schneider (6), and Moscou and Mone (7) according to the values given in Table 1.

An acid is characterized by a negative value of H_0, the most negative values corresponding to the strongest acidity. The acidity function H_0 measures the ability of the acid to give a proton to the indicator and a scale of acidity can only be established if it is independent of the indicators, which should then be chosen with the same activity coefficients.

Before 1950, the idea of relating acid proton concentration to catalytic activity in aqueous solution was applied successfully to describe the *specific*

Table 1: Hammett indicators suitable for the visible titration of colorless solids.

Indicator	Basic color	Acid color	pK_a	Acid strength/ wt% H_2SO_4
Natural red	Yellow	Red	+3.3	8×10^{-8}
Phenylazonaphthylamine	Yellow	Red	+4.0	5×10^{-5}
Butter yellow	Yellow	Red	+3.3	3×10^{-4}
4-Benzeneazodiphenylamine	Yellow	Purple	+1.5	2×10^{-2}
Dicinnamalacetone	Yellow	Red	−3.0	48
Benzalacetophenone	Colorless	Yellow	−5.6	71
Anthraquinone	Colorless	Yellow	−8.2	9

acid catalysis in dilute solutions of strong Brønsted acids in which H_3O^+ ions were the universal proton carriers (8). As physical characterization methods, such as microcalorimetry, temperature programmed desorption (TPD), magic angle spinning nuclear magnetic resonance (MAS-NMR) and infrared (IR) spectroscopy, began to be used to characterize catalysts, it became clear that the nature of acid sites on oxide surfaces was closer to *general* than to *specific* acid catalysis in solution. An attempt to improve Walling's model by including the heterogeneity of the surface acid sites within the framework of the indicator method using Benesi's amine titration technique (4) was unsuccessful, as shown in the critical analysis of Deeba and Hall (9).

Because it appears impossible for the indicators method to differentiate between the acid strengths of various Brønsted acid sites present simultaneously on a solid acid surface, other characterization methods including new physical techniques and quantum mechanical methods have been used since the 1980s to develop a novel approach for measuring and predicting the catalytic activity of solid acids.

Among all solid acids (10), zeolites are the most widely characterized and used as catalysts. They are crystalline aluminosilicates where silicon and aluminium atoms are linked through oxygen atoms, leading to a three-dimensional framework that comprises channels and cavities of molecular (0.4–1.3 nm) dimension, the latter underpinning their applications as molecular shape selective catalysts for petroleum and petrochemical industries (11,12). The challenges that zeolites have to meet for their application to the fine chemical sector have also been reviewed and discussed (13,14).

The important role played by zeolites as acid catalysts stems from a combination of properties: their role as adsorbents largely studied by Barrer (15), their molecular sieve properties initially discovered by Weisz (16,17), and their widely used ion-exchange properties (18). In particular, ion-exchange enables the generation on the zeolite of both Brønsted and Lewis acidity. Brønsted acidity can be introduced by a variety of ways, such as: (1) direct proton-exchange of the charge-compensating metal cations; (2) ammonium-exchange of the same compensating metal cations followed by calcination to decompose the ammonium cation leaving a proton on the surface; (3) exchange with polyvalent cations that can generate protons via partial hydrolysis of water molecules; and (4) exchange by metal cations that can be reduced by hydrogen to a lower valence state, again generating protons on the surface. It is remarkable that although the acidic properties of zeolites were only recognized in the late 1950s (19,20), their use as selective cracking catalysts was patented in 1961 (21,22) and described in 1964 in the journal literature (23). 90% of the US refiners and 25% of the European refiners were already using zeolites as cracking catalysts in 1969. The first zeolite-catalyzed process, based on molecular shape selectivity, selectoforming, was operated in the late 1960s at the Mobil refinery in Frontignan, France (24).

Only few types of Brønsted sites on solid acids have been established with sufficient reliability. These solids include silica-alumina, alumina, heteropolyacids, sulphated zirconia, mesoporous materials, and zeolites. The bridging OH group linking Si to Al, both tetrahedrally coordinated, in zeolite frameworks is certainly the most studied Brønsted site on solid acids and its acidic properties have been shown to depend on the zeolite structure, aluminium content, and distribution, and on the environment defined by the zeolite channels and/or cages geometry. In fact, zeolite confinement effects are of paramount importance in the definitiation of the acidity inside the zeolite pores (25).

In addition to Brønsted acid sites, zeolites can also possess Lewis acid sites; structural Lewis sites can be generated by dehydration of zeolite structures at high temperature, which leads to dehydroxylation of the Brønsted sites (26). Other types of Lewis sites have been obtained by mild steaming that dislodges Al from regular framework positions (27). In fact, mild steaming of a zeolite usually reduces the total number of Brønsted acid sites, while creating Lewis acid sites, but the remaining Brønsted sites are usually more acidic, possibly due to the interaction of extra-framework Al hydroxycations with the hydroxyl groups of normal Si(OH)Al Brønsted sites (28). This effect has very recently been observed by Niwa in a ZSM-5 zeolite (29), who reported an enhancement of the acidity of isolated Brønsted acid sites by the presence of extra-framework aluminium species, although the exact nature of these aluminium species is still unknown. The introduction, by ion-exchange, of polyvalent cations or multiply-charged species in the zeolite channels and/or cages also produces Lewis acidity in zeolites. There is even an interesting study on increasing the Lewis acidity of ruthenium nanoclusters inside zeolite cages to improve the catalytic behavior on hydrogen generation (30).

At this point it should be noted that, although our main interest in this review is related to catalysis, the surface acidity of solids is important for a wide variety of applications, ranging from adsorption (31), to sensor development (32), or even controlled drug release (33).

In the following sections we will present an overview of different methods to characterize the acidity of zeolites; these will be discussed and questioned with respect to their limitations and interpretations. The focus will be placed mainly on microcalorimetry and temperature programmed desorption using probe molecules, IR and NMR spectroscopies, the use of model reactions, and quantum chemical studies. Afterward, we will revisit the issues concerning the relation between activity and acidity.

2. ABOUT THE CHARACTERIZATION OF SOLID ACIDITY AND ITS RELATION TO CATALYTIC ACTIVITY

As mentioned above, this article will deal mostly with zeolites and the methods that have been developed for the characterization of its acidity and

catalytic properties. Before entering such a discussion, it is important to define unambiguously what is meant by the acid strength of a solid acid.

The Hammett function, H_0, has been used extensively to predict the catalytic activity of aqueous solutions (2,8). However, physical conditions in homogeneous catalysis, on which H_0 is based, are not fulfilled for acid catalysis on a solid surface and "acidity" is a concept that is often loosely referred to by catalytic chemists and chemical engineers. In fact, the term "acidity" is usually used so that it encompasses several quantities that are actually different; in particular, it is of paramount importance to distinguish between the contributions of "acid site number (and density)" and "acid site strength" for solid acids, whereas those are largely mingled in acidic solutions.

As an example, for aqueous solutions the universal acid responsible for proton transfer to a base is the hydroxonium cation H_3O^+ and all aqueous solutions have, therefore and strictly speaking, the same acid strength, i.e., the intrinsic ability of H_3O^+ to protonate a base, which can be viewed, as a first approach, as independent of the concentration of this species in solution. However, the extent of protonation of any given species in that solution will depend also on H_3O^+ concentration in solution, which depends on the concentration and dissociation constants (pK_a and pK_b) of all the acids and bases present in the solution.

A 1 M solution of HCl is more "acidic" than a 0.01 M solution of the same acid because, assuming that the acid is totally dissociated, 100 times more H_3O^+ ions are generated in the former case; this occurs despite the fact that, in both cases, we are dealing with the same acid and, thus, with the same acid strength. However, a 1 M solution of HCl is more "acidic" than a 1 M solution of acetic acid because the former is completely dissociated while the latter is not and, thus, the former yields about 200 times more H_3O^+ ions than the latter. In both cases it is likely that the protonating agent for any added base will be the H_3O^+ ion and, therefore, the extent of protonation depends mostly on the concentration of hydronium ions and not on the acid strength of the dissolved acid. The strength of the added acid, however, obviously plays a major, although indirect, role by determining the concentration of H_3O^+ ions, which depends on its relative proton transfer ability to water as quantified by its pK_a. In solution, at least in the context of *specific* acid catalysis, the solvent levels off the acid strength of acids to that of the protonated solvent, whereas the "acidity" of the medium is mainly governed by concentration of hydronium ions.

The situation is very different with solid acids. There is usually no solvent, unless the reaction is operated in liquid phase, e.g., in some fine chemical synthesis operations. The number and density of acid sites in solid acids is defined by chemical and structural parameters. Brønsted acid sites have intrinsic strengths defined by their ability to interact directly with a base, as the acid-base interaction is not mediated or the acid strength leveled off by a solvent.

In fact, IR observations have identified different OH groups on the surface of the catalysts (34); a recent study clearly identified individual OH groups of different nature, two in the supercages and two in the sodalite cages of zeolite HY (35). Another aspect that is relevant is the fact that most surfaces are heterogeneous in nature. Although we may expect all HCl molecules to possess the same acid strength, i.e., protonating ability (apart from smaller differences in solvation environment), the acid sites on a solid surface will probably possess different acid strengths, due to the fact that the acid sites will very likely have different surroundings, different structures, and locations.

Chemical heterogeneity effects may appear in zeolites not only due to the existence of different cation locations, even within the same structure, but also when partial neutralization of interacting sites is achieved either intentionally (by cation exchange or chemical reaction) or inadvertently (by dealumination) or due to defects in the crystal framework. In the compositional range where the media effect (36) plays a role, zeolites may be considered as polyacids. The general rule is that, for all polyacids, successive acid functionalities become weaker as the acid is more "deeply" neutralized. Therefore, as an example, higher pK_a values are observed for NaH_2PO_4 relative to H_3PO_4, Na_2HPO_4 relative to NaH_2PO_4, and $NaH_3P_2O_7$ relative to $H_4P_2O_7$. By analogy, a partially exchanged zeolite, such as (Na,H)-Z, should be a weaker acid than the fully protonic zeolite H-Z. It is also worth noting that $H_4P_2O_7$ is a stronger acid than H_3PO_4, the same holding for $NaH_3P_2O_7$ relative to NaH_2PO_4, as upon dissociation of the OH group, the negative charge that is left behind is better accommodated, due to its delocalization, on a larger anion, which reduces the electrostatic interaction with the leaving proton. The same holds for zeolites, where the acid strength of individual acid sites is known to increase with decreasing Al content (37), although the number of acid sites decreases. Nevertheless, this issue is still open to debate and a recent study concluded that "the progressive incorporation of aluminium in SBA-15 has a positive effect on the structural and textural characteristics of catalysts as well as on the number of Brønsted and Lewis acid sites, whereas no net effect was observed on the relative distribution of acid sites according to their nature or strength" (38), although these conclusions are not clearly visible in the results presented.

In addition to all these facts, Brønsted acid sites can also coexist and even interact with Lewis acid sites in the same solid acids, e.g., zeolites (28).

Several major difficulties arise from this situation.

- A distribution of intrinsic acid strengths can exist depending on local chemical, structural, and topological features; thus, acid strength cannot be characterized by a single number. Acid strength characterization techniques or methods need to take into account the absolute or relative amounts of sites possessing a given acid strength.

- It is difficult to establish a reliable and universal acid strength scale. In aqueous solution, a single parameter, pK_a, adequately describes the ability of the acid species to protonate water, i.e., the dissociation constant, because of the mediating effect of water acting as both a base and a solvent. A similar approach can be applied to solid acids by evaluating or measuring, using a variety of techniques, the interaction of their different acid sites with various bases. In this case, however, the base only acts as a probe molecule and it is the zeolite framework itself that acts as a "solid solvent" (14,39).
- It is necessary to distinguish between Brønsted and Lewis acid sites. As mentioned earlier, this may be complicated as they can be interrelated.
- It is also relevant to identify the location of the acid sites in the zeolite. Although this is extremely difficult in general, it is often possible to distinguish between acid sites that are located inside the zeolite pores and acid sites that reside on the outer surface by using suitably large probe base molecules (40).

3. FURTHER COMMENTS ON THE ORIGIN AND STRENGTH OF ZEOLITE ACIDITY

After the work of Barrer (41), zeolites started to be used as selective adsorbents. The discovery of their unique properties as catalysts in 1960 completely revolutionized the field of catalysis. In 10 years, zeolites became the preferred catalysts in catalytic cracking processes and were used in 90% of the catalytic cracking units in the U.S.

For most applications of zeolites, their chemistry depends on their acidic properties and shape selective effect of the channels and cages present in their structure. Acid chemistry is a dominant feature of zeolite catalysis in most of the industrial applications today. Due to the broad application and large scale on which these catalysts are used, considerable research has been dedicated towards the characterization of zeolite acidity and the kinetics of the reactions that it catalyzes.

The acidic action in various hydrocarbon reactions of Na-X, Ca-X, and Ca-A zeolites was discovered in the late 1950s (16,20,42). The fact that Ca forms of the zeolite yielded the typical products of acid catalysis is in line with the partial protonation of the zeolite due to the presence of traces of water in the medium ($Z\text{-}Ca^{2+} + H_2O \rightarrow Z\text{-}CaOH^+ + Z\text{-}H^+$). The complexity arising from the composition of the zeolites results in additional challenges for the characterization techniques and, thus, the full quantitative identification of the acidic Si(OH)Al sites in zeolites was only achieved when a material with high Si/Al ratio, but variable Al content, was eventually discovered: synthetic

zeolite ZSM-5 (MFI). Four factors determined the ability to identify these sites (43,44): (1) NMR enabling to distinguish between framework and non framework aluminium species; (2) the ability to access the same catalyst with variable aluminium concentration; (3) the choice of diffusion effect-free reactions; and (4) the quantitative determination of tetrahedral sites by cesium-ion exchange.

Protons leading to Brønsted acid sites are almost always "introduced" in the zeolite after crystallization by either direct ion-exchange or by thermolyzing NH_4^+ or other proton precursor cations. Protons, however, do not behave like the metal cations that are found in zeolite structures, as their interaction with the zeolite framework oxygen atoms resembles more a "proton attack," causing substantial changes in the bonds surrounding the newly formed hydroxyl group (45). The ability of the zeolite framework to accommodate the lattice energy resulting from this "proton attack" is a factor contributing to acid strength (36,46). A relationship exists between the T-O-T bond angles (T = Si or Al) and the acid strength of the associated bridging proton. The greater the angle is, the stronger the acid strength, as high T-O-T angles increase the strength of the T-O bond and reduce that of the O-H bond. For example, H-MOR (T-O-T angles in the range 143–180°) and H-ZSM-5 (H-MFI, T-O-T angles in the range 133–177°) are stronger acids than H-Y (H-FAU, T-O-T angles in the range 138–147°).

Brønsted and Lewis acid sites in zeolites can be interconverted. As mentioned earlier, dehydroxylation of zeolite Brønsted sites at high temperature leads to the formation of Lewis acid sites involving Si and Al sites in three-fold coordination (26). In addition, the Si-OH-Al bridge, classically considered as $Si\text{-}O^-(H^+)\text{-}Al^-$, emphasizing the ion-exchange role of the proton, could also be described as SiOH → Al, i.e., a dative coordinative bond between an electron lone pair on SiOH oxygen and a three-fold coordinated Al atom, the other resonance form (36). Considering the latter, adsorption of bases may possibly open the Si(OH)Al bridge, resembling the ammonolysis of the Al-O-P bridge for AlPO materials (47). When strong bases such as pyridine are used, one cannot exclude the possibility that an equilibrium exists between the $(Si\text{-}O^-(Py\text{-}H^+)\text{-}Al^-)$ and (SiOH . . . Py-Al) situations, which could explain why Lewis sites can still be observed by IR spectroscopy upon pyridine adsorption on perfectly crystalline zeolite materials. Obviously, all the above factors affect the quantification of the acid site nature and strength in zeolites.

Isomorphous substitutions, either by direct synthesis or post-treatment, leading to metallosilicates with zeolite structures where some of the T sites are replaced by a trivalent element other than Al, such as Ga, Fe, In, B, etc., enables the tuning of the acid strength of the catalyst. Both theoretical calculations and experimental acid strength measurements by IR spectroscopy and ammonia TPD agree on the following acidity ranking (48):

$$Al(OH)Si > Ga(OH)Si > Fe(OH)Si > In(OH)Si > B(OH)Si.$$

This order can be explained by a decreasing donor-acceptor interaction between the oxygen atom of the silanol group and the trivalent element incorporated in the structure and it has recently been obtained by density functional theory (DFT) calculations by Bao (49).

There is no doubt that the presence of extraframework Al (EFAL) Lewis acid species produced by mild steaming increases the acid strength and the catalytic activity of zeolites (28,29,44) because of the interaction between the Brønsted Si(OH)Al site and the EFAL Lewis site. Although there is an on-going debate about the exact nature of these Al extraframework species, which even in very recent works has not been unequivocally identified (29), evidence for their interaction with Brønsted sites has been obtained by IR spectroscopy in the case of H-FAU for quite some time (50). Another very recent study combined solid-state NMR with DFT calculations to study the interaction between Brønsted and Lewis acid sites and concluded that there is a definite interaction between these two types of acid sites that increases the acid strength of the sites in the zeolite framework; however, no direct interaction exists between the EFAL species and the Brønsted acid site despite their being in close proximity (51).

Framework-related effects also affect the acid strength of zeolites. Indeed, recent calculations for different structures have successfully correlated the acid strength of the sites with the computed ammonia adsorption energy (52), which has been widely used as an experimental measurement of acidity, as we will discuss below. To quantify the effect of the Si/Al ratio on the acid strength, the influence of which depends on the zeolite structure type, Barthomeuf used the concept of topological densities to evaluate the number of next-nearest-neighbor (NNN) Al sites (in up to 5 layers surrounding a given Al site) for 33 different zeolite structures. She found that the Si/Al ratio at which the protonic sites are most isolated and, hence, have the maximum acid strength varies from 5.8 (for FAU) and 10.5 (for BIK, Bikitaite) (37). Collective properties of zeolites that relate to an understanding of the environment effect on (apparent) zeolite acid strength have been interpreted as zeolites being "strong electrolytes" (36,53,54), "ionizing solvents" (55), "crystalline liquids" (56,57), and also attributed to "media effects" (36). The strong electrostatic field existing in zeolites endows them with solid electrolyte properties (53–55). Zeolites can be considered as "crystalline liquids," as all acidic protons are associated with accessible surface Si(OH)Al sites. Analogies were drawn between zeolites, other solid acids and liquid acids. It was proposed that proton activity coefficients are affected by the Si/Al ratio of zeolites (56,57). The latter proposal and the concept of topological densities (37) explain why the acid strength of zeolites goes through a maximum (the position of which is defined by topology)

as a function of Al content but do not provide parameters that relate zeolite acid strength to catalytic properties. The more recent "effective electronegativity" concept of Mortier et al. (58,59) includes both structural and compositional variables and provides such parameters.

Finally, it should be recognized that the "apparent acid strength" of zeolites (and other microporous solids) is also dependent on the structural environment within which the base or reactant will access the acid sites (39), as described by confinement effects (60,61,62,63) and the proposal that zeolites behave like "solid solvents" (14). In fact, since the molecules inside the zeolite porous framework are extremely constrained by the framework itself, one may view the molecule-framework interaction in a similar way to the solute-solvent interactions and, thus, one may consider that the molecules inside the pores are solvated by the structure and such supramolecular chemistry effects have been studied by theoretical approaches (64). In fact, some effects are also observed relating the acidity of the zeolites to the size of their crystals (65,66), introducing a further parameter in the analysis of zeolite acidity.

The conjunction of all the above factors results in a broad distribution of individual strength and density (i.e., local concentration) of acid sites in zeolites. As both structural and chemical factors are involved, it is obvious that more than one characterization technique will often be needed to obtain a valid correlation between acidity and catalytic activity. The most reliable techniques for this purpose are discussed hereafter.

We will now turn our attention to the various complementary techniques that are used to characterize the nature, strength, distribution and density of acid sites in zeolites. Their potential and limitations will be discussed in the light of the challenges identified above, as well as the ways in which the information they provide can be used to predict the catalytic activity of acidic zeolites.

4. ACIDITY CHARACTERIZATION

Zeolites are crystalline aluminosilicates based on an infinite extending three-dimensional, four-connected framework consisting of AlO_4 and SiO_4 tetrahedra linked to each other by sharing one oxygen atom. Due to that two different tetrahedra may only share one oxygen atom between them, the resulting structure is highly porous and contains channels and/or interconnected voids. Each AlO_4 tetrahedron in the framework bears a net negative charge which is balanced by an extra-framework cation.

In addition to shape and size selective catalysis, the acidic sites within the zeolite give rise to a highly efficient solid acid catalyst. When the cation is a proton, it binds itself to one of the bridged oxygens directly connected to Al, forming a hydroxyl group. A zeolite material can then be a proton donor and thus act as a Brønsted acid. There is another important type of acid sites,

where the free Al and the other compensation cations behave as Lewis acid sites. These two types of acid sites can catalyze a wide range of industrially useful chemical reactions, such as cracking, hydrocracking, alkylation, and isomerization of hydrocarbons, which by far overrules all other zeolite applications in terms of economic impact.

Catalytic properties of zeolites can be modified by ion exchange of their mobile cations, or through dealumination, changing the Si to Al ratio, or replacing Al or Si atoms of the framework by P, Ga, Fe, B, or other metal atoms (67).

Unlike most common inorganic acids, zeolites do not have a discrete distribution of acid strengths. Due to the various factors described in previous section, acid strength of both Brønsted and Lewis sites in a zeolite can vary continuously in a broad range.

For Brønsted sites, the main motives for this to happen lay on the fact that zeolites are solid catalysts and hydroxyl groups responsible for this kind of acidity are distributed all over the framework structure, in diverse microenvironments. The zeolite geometry and the atom which is in the tetrahedron centre (usually silicon) connected to hydroxyl groups are responsible for diverging stress energy, bond lengths, and angles of the structure. The occurrence of defects in the crystalline net, frequently originated by dehydroxylation and dealumination processes, can also cause local changes in the framework. All these factors combined change the bond energy between hydrogen and oxygen in hydroxyl groups, modifying their acidity.

The Lewis sites arise from the existence of compensation cations needed to keep framework electroneutrality and from the existence of extra-framework aluminium atoms with, at least, one free valence and that are usually formed in dehydroxylation and dealumination processes. They can act as Lewis acids and establish a bond to the probe molecule. These types of aluminium species were reported to occur in several oxide or hydroxide forms[1]: $Al(OH)^{2+}$, $Al(OH)_2^{+}$, AlO^{+}, $[Al_2O_2OH)^{+}$, $[Al_2O)^{4+}$, AlOOH or $Al(OH)_3$.

"The unique catalytic properties of zeolites are mainly attributed to their acidic properties. However, the characterization of their acidity is difficult because of the possible presence of both Lewis and Brønsted acid sites and the possible existence of a heterogeneous distribution of acid site strengths." (68).

4.1. Calorimetric Studies of the Adsorption of Probe Molecules

The main challenge of characterizing the acidity of zeolites consists in establishing a unique universal scale that is, at the same time, sufficiently sensitive for the different types of acid sites and easy to determine experimentally. One of the most currently used techniques consists of measuring the heat of adsorption (or desorption) of probe molecules. This is in line with the discussion presented above about the concept of acidity. In fact, acidity

is usually measured, even in aqueous medium, by the interaction of the acid under observation with a "reference" base, such as water.

Two different experimental techniques are commonly used to determine the energy of adsorption. The first one, usually designated by adsorption calorimetry, consists in keeping the zeolite sample at a constant temperature in a microcalorimeter and to introduce pulses of the probe molecule at increasing vapor pressure to titrate the acid sites from highest to lowest strength. The heat flux peak resulting from the injection of each pulse is integrated to obtain the corresponding heat of adsorption. This way, for each pulse, it is possible to determine the exact amount that was adsorbed and the energy released. Higher values of the heat of adsorption indicate stronger acid sites. The heterogeneity of acid strength that usually exists in zeolites results in a distribution of heats of adsorption. The representation of this distribution of heats of adsorption in function of the acid site coverage results in a curve that, usually, can be divided into three sections (69): (1) adsorption on Lewis acid sites (the highest values of the heat of adsorption and the lowest coverage); (2) adsorption on Brønsted acid sites (middle range values, usually corresponding to a plateau); and (3) reversible adsorption or physisorption (lowest values of heat of adsorption and highest values of acid site coverage). There are several examples of the application of the adsorption of ammonia (70,71) or pyridine (72). The working temperature must be very carefully chosen so as to minimize the physisorption of the probe molecules and, at the same time, to allow all the chemisorption sites to be filled. A more detailed description and analysis of this technique can be found in an interesting paper from Auroux (68) and in a book chapter from Mekki-Barrada and Auroux et al. (73).

A different approach was proposed by Drago et al. (74, 75) where the zeolite is dispersed into a loose solvation degree solvent, such as cyclohexane, and the heat evolved is measured upon the addition of incremental amounts of a basic probe. This technique has been applied a few times with promising results, but its application is still poorly spread (76–80).

4.2. Temperature-programmed Desorption of Probe Molecules

There is another method, designated by temperature-programmed desorption (TPD), which starts from the zeolite already saturated in probe molecules. Besides the fact that this method is based on a desorption procedure, another major difference between the previous described method and TPD resides in the fact that the temperature is changed during the experiment. This procedure is one of the most commonly used to characterize the acidity of zeolites (81). Nevertheless, it has the disadvantage of not being able to distinguish between Lewis and Brønsted acid sites and the results can be affected by the readsorption of the probe molecules on their way out of the pores (69).

TPD experiments are typically performed between an initial and a final temperature at a constant heating rate. TPD can be performed by a wide variety of methods: the heat flow curve is acquired during this process and the amount of desorbed species as a function of time is measured either the mass variation, using a microbalance (82,83), or by analyzing the outlet gas stream with techniques such as mass spectroscopy (83–86), thermal conductivity detectors (83,87), flame ionisation detectors (83), or a combination of infrared and mass spectrometry (IRMS) detectors (88). A new sensor for the detection of ammonia, based on zeolites, has been recently proposed although the comparison with conventional measurements is still unclear (89).

Although a single TPD experiment is faster because it generally uses a continuous protocol instead of a series of discrete pulses, the adsorption energy is not easily determined directly and may require a kinetic analysis of the desorption curve. The classical usage of TPD involved a succession of multiple experiments, usually at varying heating rates, that were lengthy to carry out and gave only a rather limited amount of information regarding the acid strength of the solid (84,90–93). However, several methods have been proposed to allow the use of a single TPD experiment to obtain more detailed information concerning the acid strength distribution of a zeolite, considerably reducing the amount of time required to perform a complete analysis. Since the pioneering work of Cvetanović and Amenomiya (84), several other authors have proposed different models to mathematically describe the adsorption curves, decomposing the experimental curve into their components, corresponding to quasi-homogeneous sites and resulting in the determination of the curves that correspond to the sites with different acid strengths (85,87,94–102). The area of these curves, in the case of zeolites, enables the determination of the amount of acid sites that correspond to the different acid strengths (72). In 1993, Martin et al. (103) proposed a non mathematical approach where, instead of trying to model the TPD curve, the authors proposed a different protocol for the temperature increase, introducing isothermal steps, in order to be able to isolate the desorption curves of the sites with different acid strengths. This work was later recovered and improved by Robb et al. (104).

The most commonly used probe molecule is ammonia (67,82–85,87,97,105–123). Two properties make it ideal for this kind of experimental determinations. First, the fact that ammonia is a small molecule allows it to access the narrowest pores in the structure of the zeolite, so ammonia molecules can access the entire surface of the structure and the several different types of acid sites that are available to adsorb this probe molecule. Besides that, ammonia is a strong base and this allows the building of a trustful scale of acidi stength based on its chemisorption energy. Adsorption energies between -50 and -150 kJ mol^{-1} have been reported for various zeolites prepared under different conditions (67,87,124). Shannon et al. (125) reported the synthesis of zeolites with a small amount of very strong acid sites, with adsorption energies

of −180 kJ mol^{-1} by dealumination of HY zeolites at 650°C under vacuum. The ammonia TPD curve of zeolites usually presents two peaks, indicating the existence of at least two major groups of sites with different ranges of acid strengths (81).

Other molecules are also used to characterize the acidity of zeolites in terms of adsorption energy. Among the most common are pyridine (85,115), carbon monoxide (116–118), carbon dioxide (105), water (86), and acetonitrile (119). Pyridine is also a base that is commonly used, namely in the context of IR-followed ad/desorption; it is a very strong base with adsorption energies between −90 and −250 kJ mol^{-1}, that are even higher than those obtained with ammonia but its kinetic diameter may prevent it from entering the smallest pores of the zeolite. Most of the other molecules that were mentioned are smaller but their reported adsorption energies are comparatively lower and are usually under 50 kJ mol^{-1}.

Any attempt to mathematically describe the TPD curves has to deal with the fact that the shape and location of the peaks depends on the experimental conditions under which the desorption of the probe molecule is performed (81). Although the influence of factors such as the sample mass or the heating rate can be easily controlled, phenomena such as readsorption or slow diffusion of the probe molecules present a greater challenge. These difficulties can only be overcome by combining adequate experimental conditions with the incorporation of some of these adverse phenomena in the mathematical models. Concerning experimental conditions, there are two major approaches: performing the desorption under vacuum (97,107,108,120–123) (avoids readsorption) or performing the desorption under an inert gas stream (87,106,124), typically helium or nitrogen.

We will now focus on the description of the more relevant and recent advances in the characterization of zeolite acidity based on the analysis of TPD curves.

Niwa et al. (97,102) proposed a theoretical equation that enabled the simulation of a TPD curve, which consisted in a great advance to what had been initially proposed by Cvetanovic and Amenomiya (84,90). It was assumed that once the ammonia desorbs, it can easily readsorb, because the desorption process is at equilibrium. In this method, however, because a single value of adsorption energy is obtained, it corresponds to an average of all acid sites present in the zeolite. This procedure has been applied and improved in subsequent studies (107,108,120–123). The more relevant improvement of the procedure proposed by Niwa et al. came from the combination of this technique with infrared spectroscopy. The combination of these two techniques generated a new procedure, designated as IRMS-TPD (88,120–123), which simultaneously allows the determination of the strength and amount of acid sites obtained by the traditional TPD technique, while enabling the characterization of the acid site structure. With this procedure it is possible to

distinguish between Lewis and Brønsted acid sites and individually determine their strength and amount.

A numerical method was also proposed to perform deconvolution of ammonia TPD experimental curves and to determine the strength distribution of the acid sites on the zeolite surface (87). The method assumes that for this kind of experiments, the desorption rate of ammonia from a set of acid sites with uniform energy, E, can be described by an Arrhenius-type equation.

Although it can be assumed that the distribution of acid strength of a zeolite is continuous, this model assumes that it can be represented by a discrete set of acid sites with activation energy for ammonia desorption, E^i. This method has been applied to characterize zeolite catalysts for different applications (126–128) and it was also demonstrated that the results obtained by this deconvolution method can be applied to predict the catalytic activity of zeolites for several hydrocarbons transformations, by means of Brønsted-type equations (106,129,130), similar to the ones used in acid catalysis in homogeneous phase, as it will be discussed below, when the acidity-activity relationships will be addressed.

More recently, Delgado and Gómez (99) proposed a new mathematical model for the quantitative analysis of the TPD curves in line with the one previously proposed by Gorte (100). The model is based on a set of partial differential equations, where it is assumed that the adsorption is carried-out in a well-mixed reactor and the phenomena of diffusion resistance and readsorption of the probe molecules are taken into account. The proposed model, as stated by the authors (101), presents three main problems: (1) the readsorption phenomenon is not adequately evaluated; (2) the effect of the temperature on the pre-exponential factors was disregarded; and (3) the value of the adsorption enthalpy was wrongly estimated, as a result of an existing correlation between this parameter and the pre-exponential factors in the estimation procedure that was adopted. A solution for these deficiencies was later proposed by the same authors (101), which consisted in the evaluation of the adsorption and desorption rate constants from statistical thermodynamics. Both models — the initial and the corrected ones — assume a constant activation energy of desorption so, in other words, the model assumes that all acid sites have the same strength. As a consequence, from the fitting of this model to experimental data, only one average value of adsorption energy is obtained.

Barrie (109) recently proposed some improvements to the analysis of TPD curves, when first order kinetics is assumed and the Arrhenius equation parameters — pre-exponential factor and activation energy — for each acid site are independent of surface coverage: (1) a new equation for the estimation of the critical adsorption energy, at a particular temperature, the molecules on all the sites with adsorption energies lower than the critical value will have desorbed, which is in agreement with previous work from other authors (110–114) about the adsorption/desorption of gases on/from heterogeneous

solid surfaces; (2) an equation that estimates the activation energy distribution for the adsorbed probe molecules; (3) demonstrated that the interrupted TPD experiment gives a reliable measurement of the pre-exponential factor of the peak; and (4) a new penalty function based on the square root of the second derivative, that improves the fitting to noise experimental data.

Derouane and Chang (39) raised the subject of the influence of the confinement effects in the adsorption of simple bases by zeolites. They proposed that due to the universal nature of van der Waals interaction forces, the heat of adsorption of small bases in zeolite micropores measured by calorimetric techniques is a sum of two terms. The chemical term accounts for the deprotonation of the zeolite acid center, protonation of the base, and electrostatic interaction between the negative zeolite acid centre and the protonated base, i.e., this term is the real heat of adsorption. The confinement term corresponds to the physical interactions between the adsorbed base and the zeolite framework.

The authors use data from the literature for the adsorption of ammonia, methylamine, dimethylamine, trimethylamine, ethylamine, isopropylamine, and *n*-butylamine on MFI, MOR, FER, and FAU zeolites. A model to quantify the influence of confinement effects depending on molecular size and polarizability was proposed.

Table 2 contains the experimental and corrected (for confinement effects) heats of adsorption of various bases for several zeolites presented in the literature (39).

Table 2: Comparison of the heats of adsorption of various bases ($-\Delta H_{ads}$), confinement effect energies *(CE),* and calculated heats of protonation (ΔH_{ads}-*CE)* for several zeolites (values in kJ mol^{-1})(39).

Zeolite	Base	$-\Delta H_{ads}$ (kJ mol^{-1})	$-$CE (kJ mol^{-1})	$-(\Delta H_{ads}-$CE) (kJ mol^{-1})
MFI	NH_3	145–155	18	127–132
	CH_3-NH_2	185	30	155
	C_2H_5-NH_2	195	41	154
	$(CH_3)_2NH$	205	44	161
	$(CH_3)_2$CH-NH_2	205	53	152
	$(CH_3)_3N$	205	50	155
	C_4H_7-NH_2	220	64	156
MOR	NH_3	160	26	134
	CH_3-NH_2	200	47	153
	C_2H_5-NH_2	–	65	–
	$(CH_3)_2NH$	225	69	156
	$(CH_3)_2$CH-NH_2	–	83	–
	$(CH_3)_3N$	220	79	141
	C_4H_7-NH_2	245	101	144
FER	NH_3	170–175	39	131–136
FAU	NH_3	135–140	14	121–126

Derouane and Chang concluded that the confinement factors cannot be ignored as they may represent up to 40% of the experimental heat of adsorption (e.g.. *n*-butylamine in MOR). Corrected heats of protonation, which may be related to acid strength, are only obtained when heats of confinement are subtracted from experimental adsorption heats.

Another important aspect when characterising the acidity, as it was already mentioned above, is distinguishing between the acid sites that are inside the zeolite pores and those that are located on the outer surface. It is often assumed that the acid sites inside the zeolite pores provide the major contribution to the acid-related catalytic activity of zeolites, since they are usually stronger than those on the outer surface and are also in larger amount. However, the increased interest in nanoscale particles has led to a larger proportion of outer-surface sites. In order to characterize the acid sites on the outer surface it is possible to use base molecules of sufficiently large size, so that they are not able to access the inner pores of the zeolite, such a collidine (40).

The generation of Lewis acidity is also an important issue that can be looked at by using TPD of different probe molecules. For instance, Lercher reported that, by using TPD of different molecules, well-defined Zn^{2+} sites in ion-exchanged zeolites BEA were identified (131).

Also noteworthy is the work by Manos who has applied ammonia TPD to study coked catalysts (132); coked catalysts are difficult to assess by TPD, since the desorption of coke components interferes with the measurement of the flow of desorbed ammonia, which motivated the authors to develop a methodology to circumvent this effect.

4.3. Infrared Spectroscopy

Infrared (IR) spectroscopy is a powerful tool for the analysis and characterization of zeolites and their acidity. Generally, all modes of IR spectroscopy — transmission-absorption, specular reflection, emission, diffuse reflectance, acoustic methods, etc. — can be applied (133). However, due to the simpler design of IR cells for the transmission-absorption mode, this is the most commonly used method (134). A thorough review of the literature on IR spectroscopy applied to catalytic processes by Ryczkowski (135) includes a section focusing on the various types of IR cells (with schematics and specific requirements) developed for numerous applications before 2001, namely in in situ conditions.

The application of infrared (IR) spectroscopy to zeolite samples (pure catalysts and also containing adsorbed species) dates back to the 1960s, with *operando* monitoring techniques appearing in the following decade. The advent of Fourier Transform (FT) IR equipment in the 1970s boosted the application of IR to zeolites (and other samples) due to the possibility of obtaining measurements with improved sensitivity (136). In recent decades, efforts have focused

primarily on the development of hyphenated techniques, combining IR spectroscopy with simultaneous TPD and/or MS experimental data, drastically increasing the consistency of the results produced.

Excellent reference books and review papers have been written on the subject of IR spectroscopy as a tool for catalysis (69,133,135–141), which are recommended for further reading. The aim of this section, however, is but to give a general picture of the importance of this technique for the characterization of zeolite acidity.

For zeolite acidity studies, research can be centered on the IR bands deriving from the stretching modes of the hydroxyl groups, which are responsible for the existence of Brønsted acidity. IR observations on zeolites have clearly shown that zeolites do possess different active sites; as examples, three types of acid sites have been identified in chabazite (142) and a recent study has identified at least three different families of zeolitic hydroxyl groups in MCM-22 using IR measurements of adsorbed nitriles (isobutyronitrile and pivalonitrile) and aromatics combined with microcalorimetric measurements (143). IR spectroscopy also allows the measurement of relative acidity — a recent study indicated that, within the Y zeolite family, the acid sites are stronger in USY zeolites, although HY and REY have a higher density of sites (144).

Theoretically, the higher the acid strength of the bridging hydroxyl site is, the weaker is the O-H bond and, consequently, the lower is the stretching frequency. Nevertheless, other factors, such as the chemical microenvironment (neighboring Al atoms content and proximity (140,145–149)) or the different locations in the framework, can be responsible for the existence of several distinct bands in the IR spectrum, all attributable to OH groups. This implication suggests that the hydroxyl stretching frequency is only an approximate indication of acid strength and, thus, it is not clear whether the differences in zeolite reactivity are the result of these geometric factors or of intrinsic acidity differences.

The type of coordination of the oxygen atom (terminal vs. bridging oxygen) influences the wavenumber of the O-H stretching vibration. Table 3 presents typical values of the OH stretching vibrations observed on different types of zeolites.

Table 3: Typical values of the OH stretching vibrations observed on different types of zeolites (150).

Hydroxyl group	Vibration wavenumber range (cm^{-1})
Bridging acid sites	3600–3650
Terminal silanol	3745–3750
Internal silanol	3700–3720 (isolated)
	~ 3500 (involved in hydrogen bonds)

For zeolite acidity characterization, it is also possible to use the IR technique to measure the bands originated by the adsorption of basic probe molecules. Using these probes allows the identification and, in some cases, the quantification of important parameters related to the acidity of the active sites, e.g., their nature (distinguishing between the acidic OH groups, which are the Brønsted acid centers, and the aluminium-containing extra-framework species, which are the Lewis acid centres), amount, strength, density, microenvironment, location, and accessibility. The most common probe molecules employed are carbon monoxide (CO), acetonitrile, pyridine, and ammonia (NH_3). Lercher et al. published a systematic approach to the characteristics of probe molecules used in zeolite acidity studies (131), summarized in Table 4.

Carbon monoxide is also widely used because it is a very weak base, has small dimensions which allow easy access to the zeolitic micropores, and is unreactive at low temperature (measurements are usually performed at 77 K). CO interacts with hydroxyl acid groups via H-bonding (151–156) and with cationic acid sites. The H-bond formation affects both the hydroxyl group and the CO molecule leading to shifts of the O-H and CO stretching bands (152–154). Recently, there has been a report that indicates that the H-bond formation method has to be applied with caution since O-H band splitting may not be due to heterogeneity of the acid sites but arise from Fermi-resonance effects that imply the existence of different configurations of the adsorbed species (157).

The adsorption of pyridine is particularly useful, since the characteristic IR bands of the pyridinium ion formed at the Brønsted acid sites and the coordination complexes at the Lewis sites are well differentiated at 1540 cm^{-1} and 1450 cm^{-1}, respectively (158). Because the pyridine bands are rather intense and sharp, it is possible to determine the amount of Brønsted and Lewis sites in the zeolite from molar extinction coefficients (50,159–165). It is also possible to observe bands at 1490 cm^{-1} and 1440 cm^{-1}, ascribed respectively to unspecifically adsorbed pyridine and pyridine attached to cations (166–169).

Pyridine is thermally stable up to high temperatures (170), allowing the study of the zeolite acid sites at elevated temperatures, at which the reactions of interest often take place. The main problem associated to the use of pyridine is that its kinetic diameter can prevent the probe molecule from entering the smaller pores in some zeolites. Nevertheless, this feature may be exploited to study the location of the acid sites inside the zeolite structure. For instance, the adsorption of pyridine on faujasite is responsible for the disappearance of the band at 3640 cm^{-1} assigned to the stretching vibration of O-H groups located in the supercages, but the lower frequency band at 3550 cm^{-1} assigned to the O-H groups located in the sodalite cages remains unchanged. Using pyridine and other molecules with different dimensions (e.g., ammonia, quinoline) is a frequently used strategy to distinguish between the acid sites located in the larger cages, which all molecules can access, and the smaller cages that can only be

Table 4: Criteria for the selection of probe molecules used in solid catalyst acidity studies (adapted from Lercher et al., 1996 (133)).

	Lewis acid site	Moderate Brønsted acid site	Strong Brønsted acid site
Sorption complex	Electron pair: donor-acceptor	Hydrogen bond	Ion pair (hydrogen bonded)
Detection of sorption	Shift of ν_B	Shift of ν_{OH} and changes in spectrum shape	Disappearance of ν_{OH} and appearance of IPC bands
Determination of acid strength	Correlations between ν_B shift and heat of adsorption	Shifts of ν_{OH} for a given probe	Thermal stability of the hydrogen bonded IPC
Determination of acid site concentration	Intensity of ν_B	Intensity of ν_{OH}	Intensity of IPC bands
Required spectral properties	Shift of ν_B significant compared to band half width	Absence of OH groups in the probe	Unequivocally identified IPC bands
Frequently used probe molecules	pyridine, NH_3, acetonitrile, benzonitrile, CO	benzene, acetone, pyridine, substituted pyridines, amines, acetonitrile	NH_3, pyridine (and derivatives)

ν_B – wavenumber of the characteristic vibration of the probe molecule.
ν_{OH} – wavenumber of the OH stretching vibration of the catalyst.
IPC – ion pair complex.

accessed by the smaller probe molecules. It is, however, important to consider the possibility of confinement effects exerted by the zeolite structure on the probe molecule, which depend on the dimensions of both: since zeolites act as solid solvents for molecules such as pyridine, these interactions may alter the properties of the probe and lead the same molecule to display a different adsorption behavior in different microporous systems inside the same zeolite crystal (171–173). Gil and Cejka used IR spectroscopy and pyridine adsorption to characterize the accessibility and acid strength of Lewis and Brønsted sites on MCM-58 and MCM-68 and compare them with other 12-ring zeolites (174).

Lutidine (2,6 dimethyl pyridine) was also employed, as it can detect weaker acid sites than pyridine due to its higher pKa (6.7 against 5.2 for pyridine) (175). Moreover, it may also permit to determine acid strength as ν_{8a} and ν^*(NH) bands, in the 1550–1660 cm^{-1} range, vary with Brønsted acid strength (ν_{8a} decreases and ν^* increases when acid strength increases) (176).

Ammonia is also a popular probe molecule due to its stability and its ability to differentiate and quantify both Brønsted and Lewis acid sites. However, as it is also a strong base, it adsorbs strongly and, therefore, unspecifically even on the weakest acid sites.

It should be noted that, depending on the molecule adsorbed, the structure and the activity of the acid sites may change and, thus, the acidity of the zeolite surface might be different in other conditions. Thus, the use of adsorbed molecules raises the question as to whether the results of the experiments will provide a relevant description of the acidic properties of the zeolites studied.

Infrared spectroscopy, using the far-IR region from 400 to 20 cm^{-1}, also provides a method to study extra-framework cations, which act as Lewis acid sites in zeolite structures (169,177–181).

Besides the transmission mode, IR spectroscopy applied to zeolite acidity studies is often conducted in diffuse reflectance mode (DRIFTS), due to the ease of sample preparation for these powdered catalysts and also because conventional transmission spectroscopy is not always possible to use (182), especially when in situ conditions are required (namely high temperatures and gas flows). Only two examples of this technique will be given, since the principles guiding DRIFTS are similar to those of transmission IR.

In situ DRIFTS has been used, for example, to provide insight into the mechanism of the cracking reaction of *n*-hexane over acid zeolites Beta (BEA) and ZSM-5 (MFI), following the IR bands of the hydroxyl groups and other species involved in the transformation (183).

Kazansky et al. compared data from MAS-NMR and DRIFTS of several acid zeolites and have determined the extinction coefficients of the O-H stretching vibrations, proposing to use them as a measure of the intrinsic acidity of the zeolites (184).

In recent years, developments of IR spectroscopy applied to zeolites have also been focused on combining different characterization techniques into a

hyphenated technique for the simultaneous analysis of various zeolite properties with a single apparatus. Such is the case of the combination of IR with TPD (120–123), which was previously discussed, or with in situ thermogravimetry (172,185).

4.4. Solid-State MAS NMR

Since its discovery in 1945, there has been an enormous growth in the range of applications of nuclear magnetic resonance (NMR) spectroscopy. The main factor responsible for this growth was the great increase in the sensitivity with which NMR spectra may now be recorded. These results arise, essentially, from three technological improvements: (1) the construction of superconducting magnets with very high and very uniform magnetic field; (2) the advance in computational capacities, with powerful and low-cost digital computers; and (3) the development of Fourier Transform NMR spectroscopy, replacing the initial sweep NMR spectrometers. Other facts to consider are the ingenious ways which have been developed for recording spectra entailing features such as spin-echo, cross-polarization, multiple pulse techniques, double and triple resonance, two-dimensional (2D) techniques, multiple quantum experiments and, more recently, zero-field NMR and probes for in situ experiments.

The application of nuclear magnetic resonance (NMR) spectroscopy to the analysis of solid materials had to overcome further difficulties, when compared to liquids. The fact that the species on solid samples have a very small or even null mobility causes them to present all possible directions towards the magnetic field, leading to large broadening of the signal. The possibility of anisotropic interactions, depending on the orientation of the solid crystallites in the static field can also contribute to the broadening of the NMR signal. Furthermore, in solid material, the dipole-dipole interactions are also quite strong, leading to an even greater reduction of the spectra resolution.

The solid-state NMR acquired special importance after the development of the "magic angle spinning" (MAS) probe, which transformed solid-state NMR into a high-resolution spectroscopic technique, massively used nowadays. The magic angle spinning NMR (MAS-NMR) technique was developed precisely to minimize the particular difficulties of solid-state NMR and to obtain, or at least approach, the resolution obtained for the liquid state. Basically, it consists in rapidly spinning the entire sample at a rotation of thousands of revolutions per second, to minimize the effects of the immobility of the molecules and the anisotropic interactions. This spinning is executed at an angle of 54.74° (determined so that $3\cos^2\theta - 1 = 0$ and called the magic angle) in relation to the magnetic fields to cancel the dipole-dipole interactions effect.

The application of this technique to the study of acid zeolites has mainly been done in two different areas: the determination of the structure or the location of the relevant T-atoms (silicon and aluminium) and the study of protonic

acid sites, although other areas, such as diffusion and adsorption, have also been tackled with this technique.

In the study of zeolite acidity, the most relevant nuclei studied using MAS-NMR are the ^{29}Si, ^{27}Al, ^{1}H, ^{17}O, ^{15}N, ^{31}P. These analyses have become essential in the study of zeolite chemistry, giving unique information about the nature and amount of acid sites. ^{29}Si and ^{27}Al enable the determination of the acid sites concentration, while the ^{1}H, ^{17}O, ^{15}N, and ^{31}P give information on the acid strength of Brønsted sites.

Some interesting reviews on this subject are: Thomas and Klinowski (186); Pfeifer, Freude and Hunger (187); Nagy and Derouane (188); Stöcker (189); Hunger (190,191); Ashbrook and Smith (192); Dybowski and Bai (193), Fraissard and Doremieux (194–197).

The aluminium spectrum typically presents two very distinctive peaks corresponding to both the tetrahedral and the octahedral structures (189). In this case, it is possible to determine the relative amount of the two types present in the samples from the areas of these peaks. Besides, if it is assumed that the tetrahedral aluminium atoms correspond to framework species, while the octahedral ones are the evidence of extra-framework aluminium, it is possible to calculate the ratio between both. These octahedral aluminium atoms are responsible for the formation of Lewis acid sites.

The ^{29}Si spectrum commonly observed for zeolites is composed of a series of peaks corresponding to the silicon nuclei with a different number of neighboring aluminium atoms (ranging between zero and four). Furthermore, peaks corresponding to silanol species (silicon attached to unbridged OH groups) can sometimes also be detected, even though these usually only appear in rather small amounts. The deconvolution of these spectra allows the precise determination of the relative amounts of each of the different types of silicon and, therefore, infer on the zeolite structure and aluminium distribution. Conjugating the results from both the aluminium and silicon spectra, it is also possible, based on the Loewenstein rule, to determine the molar ratio between these two elements in the framework (186,198). A clear description of the calculations involved can be found elsewhere (189). The ratio obtained corresponds to the Si and Al in the framework, ignoring the extra-framework aluminium. In some cases, the difference between the ratio obtained by the quantitative analysis of the NMR spectrum and the one obtained from the elementary analysis is substantial. These two techniques are mainly used to monitor dealumination and synthesis processes (199–205), but they can also give important information about the acidity of the zeolite.

^{17}O MAS-NMR should have an essential role in the study of zeolite acidity, because it enables the direct study of the hydroxyl groups, permitting to distinguish them from the non-protonated oxygen atoms of the framework. However, the very low natural abundance of the ^{17}O isotope (0.037%) forces the

use of expensive enriched samples, which considerably limits the use of this technique. The ^{17}O also presents a significant broadening, which can affect the resonances of this quadrupole nucleus with I=5/2 (192). Nevertheless, the use of this technique has been increasing, and it is possible to find some examples in the literature (206–210). A more detailed description of this technique and its background principles can be found in the recently published review by Ashbrook and Smith (192).

The solid-state ^{1}H MAS-NMR has been used successfully to characterize the acidity of zeolite catalysts and it was proposed that ^{1}H chemical shifts could be used as the basis of an acidity scale (124,187). Several papers concerning this subject can be found in the literature (211–214). The more unshielded protons (and that correspond to higher chemical shifts) are the protons that more easily break their bonds and, consequently, have higher Brønsted acid strength. Under these conditions, it is possible to establish an acid strength scale of protons and to determine their relative location, from the observation of the chemical shift. A list of usual shifts obtained with several zeolites can be found elsewhere (190). A typical ^{1}H MAS-NMR spectrum contains several peaks corresponding to hydroxyl groups with different surroundings. The most relevant are the bridging SiO(H)Al groups, where the proton is sufficiently acid to be catalytically active. All the water adsorbed on the zeolite surface must be removed; otherwise, a band corresponding to the water protons will overlap the ones from the protons of the hydroxyl groups. The deconvolution of the ^{1}H MAS-NMR spectrum results in the distribution (number and strength) of the acid sites (124,196) which, as recently demonstrated by Ramos Pinto et al. (124), is comparable to the ones obtained by Temperature Programmed Desorption (TPD). Another recent study has shown that it is also possible to compare ^{27}Al and ^{1}H MAS-NMR with IR spectroscopy of adsorbed pyridine (215).

^{15}N and ^{31}P MAS-NMR studies are used for in situ experiments, for which probe molecules (amines and phosphines) are adsorbed. By following these experiments with MAS-NMR, it is possible to detect protonated and non-protonated complexes, corresponding to Brønsted and Lewis sites, respectively. The differences in chemical shift result from different complexation strengths, which are directly proportional to the acid strength of the active site (216). Additional information can also be obtained by using two-dimensional MAS-NMR, where the spectra of ^{15}N and ^{31}P are acquired simultaneously with a spectrum of ^{1}H or ^{17}O (217). Another very interesting proposal is the measurement of density of acid sites, including the effective distance between two acid sites, using diphosphines as probe molecules (218) or by direct analysis of NMR spectra (219).

Fărcaşiu and Ghenciu proposed an interesting method of measuring zeolite acidity by ^{13}C NMR spectroscopy, in which unsaturated ketones are used as indicators (220).

Recent advances in NMR, namely flow-through probes, which enable operando conditions, combined with hyperpolarized ^{129}Xe result in higher resolution spectra and faster signal acquisition (185). This new generation of ^{129}Xe has potential to substantially contribute in the study of the porosity and the associated diffusion phenomena that are determinant in zeolite acidity.

A very recent paper reports the use of ^{1}H and ^{27}Al DQ-MAS NMR spectroscopy to observe the synergic effect between Bronsted and Lewis sites (221), an issue we will refer to again. Also recently, the motion of protons within the zeolite porous network was inspected by ^{1}H MAS-NMR (222). In fact, MAS-NMR is a particularly well-suited technique to investigate transient phenomena and it is worth noting the work by White on the study of the transient acidity that may be observed in some zeolites (223); this study reveals the dynamic nature of acid sites in zeolites.

MAS-NMR has also been used to detect the presence of reaction intermediates and analyse reaction mechanisms. For instances, Wang resorted to ^{13}C-MAS-NMR to analyse the reactivity of surface alkoxydes produce n zeolite acid sites interacting with methanol (224). A recent review covered the use of NMR techniques for the elucidation of reaction mechanisms in heterogeneous catalysis (225) and we will not go into further details in this article.

4.5. Model Reactions

The physicochemical techniques referred to in the previous sections are usually employed under special conditions, which are considerably different from the ones used in catalytic reactions. As a consequence, sometimes the characterized surface may not be the active surface. Apart from that, the heterogeneity of the acid sites may induce observable differences between what can be measured using a characterization technique and what is measured during the catalytic process itself, as Knözinger reported (226). When characterizing the acidity of zeolites using model reactions, this problem is avoided, offering not only an efficient method to control the quality of industrial catalysts, but also an efficient way to characterize the strength and density of the acid sites.

The major problem that is raised when using this methodology is that there will be no single reaction that can be used to characterize the acidity of a zeolite sample, since each reaction has its own sensitivity towards the different aspects of acidity — some will be more sensitive to acid strength, others to acid site number and density, and still others to acid site accessibility; so, this methodology will have to rely on a number of reactions that can offer the complete perspective. There is a significant number of compounds which can be used as model reactants and the best reactions must be chosen considering the structure of the zeolite, strength of its acid sites, and purpose of the comparison. In order to be used, the reactions must have a simple mechanism and present an easily measurable initial rate.

This method presents the advantage of, in principle, allowing the distinction between Brønsted and Lewis acid sites, instead of the usual determination of the total number of sites. The Lewis acid sites alone do not seem to be active in most hydrocarbon reactions, although their coupling with Brønsted sites results in a great increase of the activity, especially in double bond shift and cis/trans isomerization of olefins (227).

The characterization of the strength of the acid sites is achieved by providing a relation between the rate of reaction and the acid strength. To obtain this relation, one can use two different procedures; by measuring the acidity of a series of solids differing in the strength of their acid sites or rather of only one solid, the acid sites of which have been selectively poisoned to different extents.

Guisnet et al. (228), using the second procedure, established, for a wide range of reactions, the change in the activity of protonic acid sites as a function of their strength. The reactions in Table 5 were chosen considering the following criteria.

1. The reactions are known to occur through catalysis on protonic acid sites without participation of basic sites or of Lewis sites.
2. The reactants or the products do not cause any modification of the catalyst acidity.
3. The reactions differ considerably on their rate, requiring sites of very different strengths for their catalysis.

The catalyst used was a stabilized HY, presenting protonic sites of very different strengths. Pyridine was used to poison the acid sites.

Table 5: Reaction temperature (T_R) and type of reaction for several selected compounds (228).

Reactant	T_R (K)	Reactions
3,3-dimethyl-1-butene	473	Skeletal rearrangement
cyclohexene	473	Skeletal isomerization Hydrogen transfer[1]
2,2,4-trimethylpentane	623	Cracking
2,4-dimethylpentane	623	Isomerization Cracking
2-methylpentane	673	Isomerization Cracking
n-hexane	693	Isomerization Cracking
o-xylene	623	Isomerization Disproportionation[1]
1,2,4-trimethylbenzene	623	Isomerization Disproportionation[1]

[1]Bimolecular.

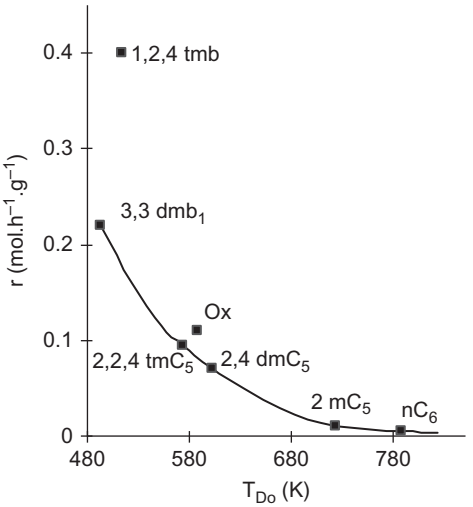

Figure 1: Transformations of various hydrocarbons on a stabilized HY zeolite. Reaction rate (r) vs. acid strength required. T_{Do} = minimum temperature of pyridine desorption for measurable rate. nC_6 = *n*-hexane; $2mC_5$ = 2-methylpentane; $2,4dmC_5$= 2,4-dimethylpentane; $2,2,4tmC_5$ = trimethylpentane; ox =*o*-xylene; 1,2,4tmb = 1,2,4-trimethylbenzene; $3,3dmb_l$ = 3,3-dimethyl-1-butene (adapted from (228)).

The series of reactions presented in Table 5 were classified as a function of the minimum acid strength in order for a site to be active, which was estimated by determining the lower temperature of pyridine desorption which enables the measurement of the activity. The value of T_R clearly depends on the reaction, ranging from 473 (3,3-dimethyl-1-butene isomerization) to 693 K (*n*-hexane transformation). The results obtained for the various reactions are presented in Fig. 1.

From Fig. 1 it is possible to conclude that the lower the desorption temperature of pyridine, the faster the reaction is. The method proposed by Guisnet et al. has the advantage to allow the distinction between Brønsted and Lewis acid sites. A more detailed description of this method can be found elsewhere (227,228).

Yoneda (229) proposed a method he called "regional analysis," which allowed to determine not only the acid strength of the sites, but also their distribution. The protonic strength of the acid sites, estimated by the Hammett acidity function (2) values, is classified according to its intrinsic activity in a series of catalysts. This method presents the disadvantage of not distinguishing between Brønsted and Lewis acid sites. In order to overcome this limitation, Guisnet et al. proposed a new method (228), where the desorption of pyridine is followed by infrared spectroscopy, enabling to quantify the number of acid sites that are regenerated. They consider that the average turnover number value of protonic sites (N) between T_{D1} and T_{D2} is expressed by the inverse of the ratio between the change in the number of protonated sites

(Δn) and the activity resulting from it (ΔA). The distribution in strength of the Brønsted sites can be established determining the values of N for several intervals of T_D and for several reactions. The main limitation of this technique is that it is only valid when the activity depends exclusively on the strength of the acid sites and not on their density, which usually is only true for monomolecular reactions.

As referred previously, besides strength, another important parameter in the characterization of the acidity is the density of acid sites, especially in the case of some bimolecular reactions (requiring more than one active site). In these cases, the final activity is the result of the combination of these two factors: strength and density.

The density of the acid sites, i.e., the distance between them, can be estimated by the ratio of the rates of a bimolecular reaction (requiring more than one acid site) and of a monomolecular reaction (requiring isolated sites with similar acid strength).

Guisnet et al. (228) presented an example of the application of this method, using two HY zeolites, with Si/Al ratios of 3 (HY3) and 35 (HY35). The reaction chosen was the cracking of *n*-heptane at 623 K. The product distribution obtained in both cases was different, indicating that the reaction followed completely different reaction pathways. When catalyzed by HY3, the reaction follows a classical carbenium ion mechanism, but in the case of HY35, light fractions are obtained (C_1 and C_2), indicating a monomolecular mechanism with a carbonium ion as intermediate.

Kramer et al. (230) proposed the use of the selectivity of the isomerization of 2-methyl-2-pentene as a probe for acidity. This reaction has the particularity of combining a double bond shift, which requires low acid strength (thus occurring in almost all the acid sites), with a methyl shift, which is much more demanding in terms of acid strength. The conjugation of these two mechanisms enables the characterization of the acid strength of the active sites. The double bond shift acts as a normalization of the site density, since it occurs in almost all the active sites. As a consequence, the selectivity of the methyl shift relative to the double bond shift gives a measure of the site strength. The main advantage of this reaction is that it involves only one reactant, enabling to correlate the acidity with the selectivity, instead of the rate.

A recent study by McVicker et al. proposes the use of methylcyclohexane ring contraction as a probe reaction that is sensitive to both the number and strength of the acid sites in solid catalysts but also to shape selectivity effects (231).

4.6. Other Methods

Other techniques can be used to analyse the acid-base properties of zeolites. Reverse gas-chromatography has been successfully used to characterize the acid-base properties of MgY and NH_4Y zeolites using a variety of

molecular probes (232). This technique allows the use of both polar (acetone, thf) or non polar (n-hexane, n-heptane) probes.

Micro-spectroscopy has also been used, in operando conditions, to analyze the acidity of zeolite samples (233); in this work, a combination of in situ optical, fluorescence, and synchrotron-based infrared microscopy was used to visualize the product distribution inside a zeolite crystal, as well as their alignment within the pores. Microspectroscopy techniques are becoming increasingly interesting to analyze phenomena at microscopic level, in particular acid-catalyzed reactions. In fact, a recent work has applied UV-Vis and confocal fluorescence microspectroscopy coupled to model reactions to study Brønsted acidity and catalyst deactivation at the individual particle level (234,235) and Weckhuysen reported the detection of carbocationic species within large ZSM-5 crystals using UV/Vis and IR spectra (236).

Another very recent study used UV-Vis microspectroscopy, scanning transmission X-ray microscopy and a model reaction (4-fluorostyrene oligomerization) to evaluate Brønsted acidity differences within zeolite materials at the nanoscale (237). A similar model reaction was used in conjunction with integrated Laser and Electron Microscopy (iLEM) to correlate acidity and structure in FCC catalysts (238).

UV-Vis spectroscopy of an adsorbed dye has also been reported as a way to measure both the internal and the external acidity of zeolites (239). Neutron and X-ray diffraction have also been used to inspect Brønsted acid sites. This technique is rather more elaborate and involves the deuteration of the acid sites prior to diffraction experiments (240).

We should note that increasing insight can be gained by combining a variety of techniques. An interesting study has been recently published by a relatively large team of authors who combined atomic force microscopy (AFM), high-resolution scanning electron microscopy (HR-SEM), focused-ion-beam scanning electron microscopy (FIB-SEM), X-ray photoelectron spectroscopy (XPS), confocal fluorescence microscopy (CFM) and UV/Vis, and synchrotron-based IR microspectroscopy to investigate the dealumination processes of zeolite ZSM-5 upon steaming at the individual crystal level, in particular in what concerns the acidity of the samples (241); the conclusions reached are in accordance with the usually accepted effects — mild steaming resulted in an enhanced acidity and reactivity, while harsh conditions improved the accessibility by generating mesopores and severe dealumination resulted in a significant loss in acidity and, consequently, in activity.

5. MOLECULAR MODELING OF ZEOLITE ACIDITY

With the increase in computation power available, molecular modelling methods based on quantum chemical principles are developing as useful and powerful tools for the simulation of the structure, properties, and behavior of

organic and inorganic chemical compounds. These techniques are increasingly allowing the catalysis community to gain insight into the structures of catalysts and the mechanisms of catalytic processes (242).

The application of molecular modelling to the zeolite field already proved to be very useful in investigating important aspects, such as the formation (243), structural, and acidic properties or the determination of the interaction of zeolites with hydrocarbons and other molecules, as well as to evaluate and develop mechanisms that can explain reaction pathways in the transformation of substances on zeolitic surfaces (244,245). A recent review has been published on the use of computational methods of inorganic solids which covers extensively the more recent work (246). A very recent study by Shaikhutdinov et al. has used DFT calculations to analyze the formation of preparation of well-defined aluminosilicate thin films (247).

Several different types of theoretical models are available: the molecular mechanics models are not too accurate but are extremely fast; the semi-empirical methods appear as an intermediate approach and the ab initio and derived methods that come very close to reality but are very time-demanding methods. More recently developed density functional theory (DFT) methods, adapted from the ab initio methods, has developed as a signifficant alternative, due to the fact that these are still very accurate but have a substantially diminished computational time. The most important factor to account for, while choosing the appropriate method to perform a specific simulation, is the relation between time and exactness that is intended.

Semi-empirical, ab initio, and DFT methods result from quantum mechanics calculations. Ideally, the true solution for this kind of problems should arise from the solution of the Schrödinger equation. However, this equation has never been solved analytically for multi-electron systems. In order to find a solution, some approximations must be made. Specifically, it can be considered that the wavefunction of a multi-electron system is the product of all the single-electron wave functions. This is called the Hartree-Fock (HF) approximation. The ab initio methods are the ones that appear directly from the application of this approach.

Because the HF approximation considers the electrons as independent entities, electron-electron interactions are not correctly estimated, since the electron correlation is ignored. This kind of approximation induces significant errors and is not too reasonable for describing hydrogen bonds, particularly when the main purpose is to investigate the Brønsted acid strength in zeolites. It is convenient to use methods that already contain electron correlation to correct this effect. The Möller-Plesset methods, for instance, includes corrections for the classic HF model and also takes into account the van der Waals interactions but, on the downside, they are very expensive methods in terms of computational effort.

On the other hand, the DFT methods were developed to substantially minimize the calculation times. The innovation in these methods consists

in replacing the electron exchange term of the HF models, which basically accounts for the electron-electron interactions, with a function that depends on the electronic density distribution. The introduction of this modification speeds up the calculation time without losing exactness. Furthermore, the use of the electronic density on the DFT models automatically establishes some electron correlation to take into consideration the electron-electron interaction that is ignored in some of the simpler ab initio models.As the computational power increases other, more advanced methods which also include electron correlaction, such as the Moller-Plesset methods, are being used. A recent publication compares calculations on the adsorption of small alkane molecules in purely siliceous and protonated chabazite at different levels of theory (248).

Semi-empirical models also originate from the HF approximation, but establish a few simplifications to the ab initio models and, at the same time, introduce several empirical parameters. Altogether, this feature substantially reduces the calculation time but at a considerable cost in terms of accuracy.

5.1. Modeling the Active Site

One of the most important aspects when modelling a zeolite is how to model the structure and catalytic site. In order to produce accurate simulations of the structure, a large number of atoms has to be employed, which severely limits the application of accurate methods. However, in order to simulate the active site, disregarding the possible confinement effects, it is possible to construct smaller clusters.

In the current article we are particularly interested in the aspects concerning acidity and several studies have been carried-out involving both Brønsted and Lewis acidity (249–251).

DFT methods have been used to study the distribution of Al and, consequently, of the Brønsted acid sites, on MCM-22 (252) and Y zeolite (253). A very important aspect that has been recently investigated is the acid sites in H-FER zeolites with different Si/Al ratios, concluding that there are different types of sites and that these depend on this ratio (254,255).

Another effect that is commonly accepted — that EFAL species enhance the acidity of Brønsted sites (51) — has also been investigated by DFT, concluding that hydrogen bonding of the hydroxylated EFAL species with the conjugated base of the site contributes to an increase in its acid strength (256,257).

More exotic effects, like the mechanism of nitrogen substitution to produce nitride zeolites, has been investigated by Auerbach, concluding that nitride zeolites should be stable (258).

Calculations on isomorphic substitution in zeolite structures have also been performed. Recent studies on the acid strength of OH groups associated with silicon or with other atoms have calculated deprotonation energies for Si-O-H and V-O-H in redox model silicate zeolites and concluded that the former

are less acidic than the latter (259,260). Regarding Lewis acidity other studies, involving the use of periodic DFT approximations, predicted the presence of Lewis acid base pairs in Nb and Ta dehydrated zeolites (261) and on B and Ga substituted LTL zeolite (262). A very recent report indicates that the high acidity of zeolite acid sites is due to an intermolecular solvent effect that enhances the acid strength of the sites (263).

DFT methods have also been used to analyze the framework basicity of zeolite frameworks (264), a complementary property to zeolite acidity.

5.2. Simulation of the Adsorption of Molecules

The adsorption of molecules is a very important feature in the chemistry of zeolites. The principal industrial applications for these materials are the separation processes by selective adsorption of molecules and the catalysis of chemical reactions. While, for the first application, the importance of the study of those phenomena is obvious, for catalysis the adsorption processes play a less evident role but just as important nonetheless. The reaction mechanisms over zeolites involve the adsorption of the reactants on the active sites of the surface and desorption of the products after the reaction step. For these reasons, the adsorption steps can contribute to the overall reaction rate, as much or even more than the reaction itself. Furthermore, if the interaction between the zeolite active site and the adsorbed reactant is sufficiently strong, the activation energy can suffer a drastic decrease. If so, the activation of the complex formed during the adsorption process can largely influence the rate of the reaction.

It is also possible to use molecular modelling techniques to evaluate the strength of acid sites in zeolites. Two major methods can be used: the determination of the energy of adsorption of probe molecules and the determination of the proton affinity of the deprotonated Brønsted sites. The studies of the interactions with probe molecules have as their main advantage the fact that results achieved through these methods can be directly compared with experimental data obtained by calorimetric or infrared spectroscopy studies. The type of sites used in this kind of studies are Brønsted acid sites because they are, by far, the most common active sites in zeolites and their nature and structural arrangement are well known.

After choosing the best numerical method for the desired accurateness, the key factor in the use of the molecular modeling of zeolites consists in deciding what the best molecular structure to describe the active site is. Several different approaches have been employed but the types of structures can be divided in two main groups: the cluster approximation structures (265–276) and the embedding models (277–279). While the clusters are simpler structures with only a few T atoms and can only be used to evaluate the direct interaction of the probe molecule with the site itself, the embedding structures are larger models

that can reproduce more realistically the structure of a zeolitic cage. These last methods allow simulating the entire environment involving the adsorbed molecule and the interaction between it and the far atoms of the structure. In some cases, this influence can be almost negligible but, especially for large adsorbed probes, it should not be neglected. Obviously, this scheme generates a much more correct approach but, as expected, the computational time is considerably increased. On the other hand, some hybrid methods can be used. In these cases, the entire zeolite cage is simulated but, for the distant atoms of the lattice, only the electrostatic contribution, based on the potential function, is calculated. A recent study compared different models for the adsorption of different adsorbates on ZSM-5 concluded that extended-cluster models offer an attractive alternative to periodic simulation (280).

Inclusion of dispersion effects are also very important, as observed in computations on CO_2 adsorption on different zeolites (281). Another important factor is the selection of the most appropriate relaxation scheme. To choose between rigid models, where the atoms in the lattice are frozen in fixed positions, and relaxed structures, where part or all of the atoms are not constrained and their positions are able to change during the geometry optimisation process, is again a compromise between the computational time and the desired correctness of the results. The starting point for the construction of the models of the zeolite lattice is usually the geometrical data obtained by experimental methods, such as XRD spectroscopy. Nevertheless, with the use of fully relaxed models, it is possible to determine an estimate of the optimal structure of a zeolite cage that can be used to study the interaction with the probe molecules.

By analogy with the experimental calorimetric studies, ammonia is, beyond doubt, the more frequently used probe (266–271,277–279). This happens because the most important information that can be extracted from this type of simulations is the adsorption energies, so it is important to have large amounts of experimental data that can be directly compared with the calculated figures. Nevertheless, other molecules, such as water (272,273), carbon monoxide (274,275), and methanol (270) are also widely used. A very recent study used a DFT model to compute NMR spectra for adsorbed acetonitrile as a probe to measure the acid strength of zeolite sites (282).

Another way to obtain information about the Brønsted sites is through infrared spectroscopy. This technique allows the characterization of the OH groups of the zeolite and the associated stretching frequencies in the presence or absence of adsorbed molecules. This data can be directly related to the bond energy between the hydrogen and oxygen atoms and, thus, can be used to evaluate the acid strength of the sites. It is possible to determine the vibrational frequencies by theoretical calculations using quantum chemistry methods; nevertheless, correction methods to solve the problem of anharmonicity of the hydroxyl groups must be applied to obtain realistic results.

Another interesting on-going discussion in quantum chemistry is to determine exactly how the adsorption mechanism is, particularly if the adsorbate can form hydrogen bridges with the oxygen atoms of the zeolite framework. As shown in the examples of Fig. 2, for ammonia, for instance, the molecule can form only one bond through the acidic proton (Fig. 2, structures A and B) but, on the other hand, if there are hydrogen atoms capable of forming bridges, one or more extra bonds can be formed between the adsorbed molecule and the zeolite (Fig. 2, structures C and D). Evidently, this hypothesis leads to a more stable configuration and, as a result, to greater adsorption energy. On the other hand, it is also important to realize if, during the adsorption, the acidic proton remains connected to the zeolite framework, forming only a hydrogen bond with the ammonia molecule (Fig. 2, structures A and C) or if there is a proton transfer to the adsorbate, forming an ammonium ion (Fig. 2, structure B and D). Several studies have shown that this last assumption corresponds to a more stable structure (267,278). However, Kassab et al. (271) showed several examples where opposite results were obtained for the same cluster models, only by the use of different numerical methods. This demonstrates how important and relevant the choice of a particular numerical method can be.

Recent works have been able to simulate the desorption curves obtained in experimental TPD runs using ab initio computed potentials (283).

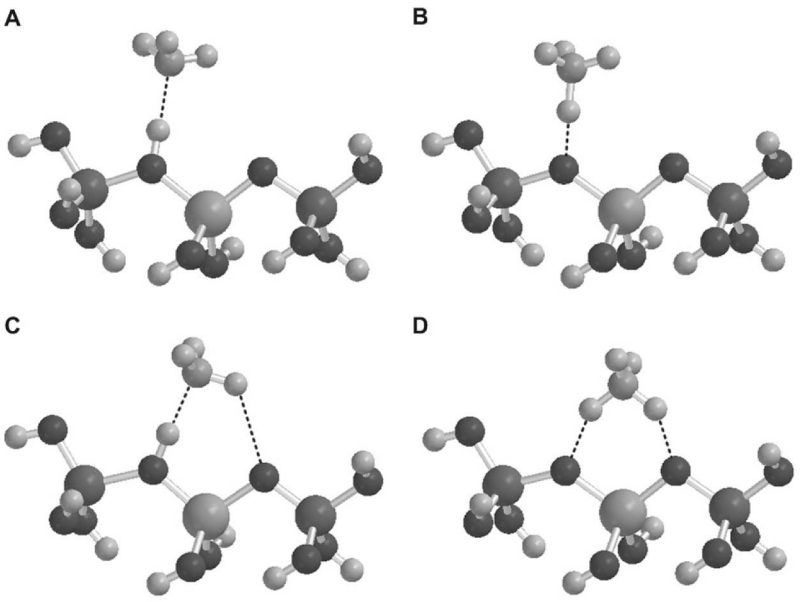

Figure 2: Different structures for the adsorption of ammonia in a $(OH)_3SiOHAl(OH)_2OSi(OH)_3$ cluster. The first two structures correspond to adsorption on a single site by a neutral complex for structure A and by an ionic complex for structure B. Structures C and D correspond to adsorption on two sites simultaneously in the neutral and ionic forms, respectively.

DFT calculations were used by Curtiss to analyse the adsorption and diffusion of fructose in zeolite HZSM-5 (284), concluding that the reaction thermodynamics cannot be predicted correctly using small cluster models because these fail to represent the electrostatic effect of a zeolite cage, which provides additional stabilization upon the protonation of fructose.

5.3. Determination of Deprotonation Energy

The determination of the deprotonation energy (i.e., the proton affinity) of the Brønsted acid sites is one of the possible ways of characterizing the acidity of zeolites. The main problem with this methodology consists in the difficulty of experimentally measuring this quantity. Datka et al. (285) presented a method to determine the deprotonation energy by infrared spectroscopy through the adsorption of different bases. Nevertheless, this method is more complicated and time-demanding than the calorimetric or TPD techniques. Moreover, the results can also be less reliable compared with standard methods and, if so, the best way to determine it is by using the theoretical models and quantum chemistry calculations. In fact, in the last few years, the considerable increase of the calculation capacity of computers has made theoretical modeling more accessible and, consequently, more generally used. Several studies can be found in the literature, using the wide range of theoretical methods referred to previously (267,269,276).

A recent study has compared the use of deprotonation and protonation energies, by resorting to DFT calculations on group V Al containing zeolites, and concluded that protonation energy is a better descriptor for acid strength than deprotonation energy (286).

The main disadvantage of this method is the difficulty in comparing the values obtained using molecular modelling with experimental values, which would give an idea of the degree of accuracy of those models. The type of acid centre selected can also influence the final values, as explained before.

It has been shown by Brand et al. (267) and Wang et al. (269) that there is a linear relationship between desorption energies of ammonia and the deprotonation energy for the same site using the same theoretical method. A similar conclusion was reached by Su and Vercauteren who obtained an acidity order for different zeolites using periodic DFT calculations (287). Yáñez et al. also related the deprotonation energy with the adsorption energies of different bases, concluding that stronger bases tend to form ion pairs when interacting with the acid site (288).

The fact that the calculation of adsorption energy of bases is closer to experimental determinations and all the factors discussed above discourage the use of the determination of deprotonation energy in favor of the energy of adsorption of probe molecules (especially ammonia) to establish an acid strength scale for zeolites.

However, it should be noticed that quantum calculations also allow the study of processes like proton mobility. Sauer reported calculations on the proton jump between two adjacent oxygen atoms in the zeolite framework that compared well with the same property measured by NMR (289).

5.4. Reaction Mechanisms and Acidity-Activity Relationships

The study of reaction mechanisms by quantum chemical models is also a very important area of development. Quantum chemical methods allow the calculation of both stable species and transition-state intermediates and to analyse the reaction coordinates.

Several studies have been performed on the mechanisms of reactions over zeolites. The transformation of ethane (290) and propene (291) over zeolites and its relation with acidity was studied using HF/6-31G** theoretical model and for propane (269) and n-hexane (292) using a HF/DFT B3LYP/6-31G** model. In all cases, it was observed that the computed activation energies for the main reaction correlated linearly with the heat of adsorption of ammonia computed using the same theoretical model. This gave a theoretical support for the development of Brønsted-type relationships that were used to interpret experimental data, as it will be discussed below. Deng recently published studies that, as expected, concluded that the activation barrier for the dimerization decreased as the acid strength increased (293,294). In the case of the dimerization of ethane (294), using a ONIOM (B3LYP/6-31G(d,p):MNDO) model the authors also analysed the confinement effects and concluded that the zeolite structure stabilizes the activated states. Confinement effects have, indeed, been studied by computational models and a recent publication rationalized the confinement effects as being connected to electrostatic stabilisation of the species inside the porous network, which is of particular importance when charged intermediates are generated, and to the existence of space limitations and rotational mobility of the encaged molecules, which may introduce transition-state shape selectivity effects, but also to the "breathing" movements of the whole zeolite structure, which are deemed as a driving factor behind ring-contraction reactions (295). Mota et al. computed the energetics of the ter-butyl cation inside zeolite Y (296), concluding that this carbocation is stable within the zeolite framework. Confinement effects have also been analysed, using DFT calculations, in relation to Sn Lewis acidity in zeolites, concluding that the nature of the site is strongly dependent on the zeolite framework structure and on the environment of the specific site (297).

Louis et al. reported a detailed study, coupling experimental data and an ONIOM/B3LYP theoretical model to study the partial oxidation of benzene by N_2O over H-ZSM-5 (298); from the results obtained they suggested that the reaction proceeded by a Langmuir-Hinshelwood-type mechanism between benzene and adsorbed N_2O; additionally, two distinct active sites were identified.

A study on the disproportionation of N_2O_4, also using a DFT theoretical model, has also been reported (299). Corma et al. reported a theoretical study on the carbonylation of methanol and dimethyl ether with CO on Mordenite, evidencing the action of different active sites (300,301).

DFT calculations were also used to support an experimental study on styrene oligomerization as a molecular probe reaction for zeolite acidity, concluding that the preference for a particular reaction mechanism is determined by the local shape of the zeolite micropores (302).

Bucko et al. reported a DFT study on the protolytic cracking of propane over acidic chabazite and, using a semiempirical dispersion correction to account for van der Waals interactions between propane and the zeolite, they obtained adsorption energies that compare well with experimental values (303); they also obtained results indicating that stable reactant complexes with Brønsted sites occur only at low temperatures, in agreement with the observed reactivity.

Pidko reported a comprehensive study on the activation of light alkanes over Zn-exchanged zeolites, applied to the dehydrogenation of ethane (304); the authors identified different Zn sites, concluding that a particular type of sites most favors the reaction. They also concluded that the proximity between Brønsted acid sites and the Zn Lewis sites promotes the catalytic cycle, once again reinforcing the idea that a synergistic effect exists between the Brønsted and the Lewis sites. Another DFT study focused on Fe sites in ZSM-5 for the oxidation of benzene to phenol (305).

Duca et al. performed calculations, at a DFT B3LYP level, on the isomerization of butane using a model for a ZSM-5 cage with and without Pd atoms adsorbed and concluded that the reaction occurred via a π interaction between the olefin and the acidic sites and that the activation energy of the Pd-containing zeolites was lower than if the reaction occurred on a bare Pd surface (306).

Janik and Song reported equilibrium calculations on the ring-shift isomerization of sym-octahydrophenanthrene to sym-octahydroanthracene using an ONIOM approach as a way to support experimental data on this reaction (307). DFT was used to support their studies on the oligomerization of glycerol (308) and ethyl chloride conversion (309) on acidic zeolites. The methanol to gasoline reaction has also been analyzed using DFT models (310).

An interesting note is that some authors have reported apparent violations of the usually accepted rule that implies that higher acid strength should result in higher activity; using an ONIOM2 (B3LYP/6-31G**:AM1) theoretical level, they observed that the introduction of sodium cyclopentadienyl in a HMCM-22 zeolite resulted in a lowering of the acid strength that was accompanied by a lowering of the activation energy for the protonation of ethane as well (311). This was attributed to the interaction of the CpNa moiety with the proton from the acid site but no experimental support is given.

A very important aspect when dealing with reaction mechanisms is the ability to correctly estimate activation barriers. Sauer reported the use of a combination of MP2 with periodic DFT which is shown to provide, for the methylation of light olefins, estimates of activation barriers that agree well with experimental values (312).

Van der Mynsbrugge et al. also reported the estimation of reaction rate constants for the methylation of benzene by methanol using a two-level ONIOM(B3LYP/6-31+G(d):MNDO) method (313); the estimated rate constants compare well with experimental ones for ZSM-5 althoguh large differences were obtained for Beta zeolite. Nevertheless, this recent study indicates that quantum chemical methods are rapidly approaching the ability to estimate usefull kinetic parameters.

6. RELATION BETWEEN ACIDITY AND CATALYTIC PROPERTIES

We can say that the Holy Grail for catalysis would be the ability to correlate the characterization of the catalyst with its catalytic performance. The final goal would be to predict the catalytic activity based solely on characterization results. Correlating reaction kinetics with thermodynamic parameters, such as the acid strength of a site, has been a goal for a long time. In 1995, Hammond wrote "Chemists have long been plagued by the lack of any general correlation between reaction rates and the positions of chemical equilibria" (314).

In order to be able to relate acidity with activity, one has to take a look at the type of reactions that are catalyzed by these acidic solids. Zeolites are often involved in acid-catalyzed reactions, where a carbocationic intermediate is formed. Therefore, the chemistry of the reactions is closely related to the chemistry of the carbocation, which can be divided into four major steps: (1) formation of the carbocation from the reactant through the adsorption on the acid center; (2) conversion of the carbocation of the reactant to that of the product; (3) hydride abstraction by the product carbocation from a molecule of starting material; and (4) termination step with loss of cationic state.

Carbocations can easily be formed by protonation of alkenes or aromatics on the Brønsted acid sites of the zeolite. The mechanisms followed have been widely studied and it is generally accepted that the carbocation is formed through the classic mechanism of organic chemistry.

On the other hand, formation of carbocation for alkane reactions has been causing some controversy. Initially, it was proposed that the carbocation was formed by hydride abstraction, following the classical mechanism of organic chemistry (intermediary called carbenium). Following Olah's proposal, there is a mechanism where protonation of the alkane forms a non classical carbocation (carbonium). The intermediate formed is a weakly coordinated species where there is a pentacoordinated carbon atom and a non-localized charge

(269,315–319). This non classical carbocation is not a thermodynamically stable species (corresponding to a local minimum on the potential energy surface) but a transition state called carbonium.

The classical mechanism of catalytic cracking has difficulty in justifying the formation of products with only one or two carbon atoms. Through this mechanism, the formation of these species would involve the formation of a primary carbocation, which is extremely unfavored by kinetics. However, through the carbonium theory, it is possible to justify the formation of those smaller cracking products that are effectively observed experimentally. The formation of neopentane must also occur through formation of the pentacoordinated species, due to the fact that the formation of a carbocation by abstraction of a hydride ion from this paraffin is highly unfavored (320). This theory has been supported by experimental evidence, obtained by Haw et al. using ^{13}C MAS-NMR spectroscopy (321,322).

Quantum chemistry modelling at different levels of theory was used to test the carbenium theory; supporting data have been obtained by several authors (323–327), although data have also been provided to support a carbonium mechanism (327,328) and Corma has recently published an article where he concludes that "on a zeolite surface, most of these species do not exist as free carbenium ions, but are covalently bonded to framework oxygens" (329). The non classical adsorbed carbonium undergoes a protolytic cracking forming an alkane and a smaller carbenium ion. The nature of these species is still relevant today and, as mentioned above, only recently an article reported the detection of carbocationic species inside large zeolite crystals by synchrotron-based IR microspectroscopy (236).

An adsorbed carbenium can undergo one or several of the following reactions: it can desorb as an alkene by giving back a proton to the zeolite; isomerize to a more stable configuration; crack through ß-scission forming a smaller carbocation and an alkene; go through a cyclization; and/or react with an alkene or an aromatic yielding a longer carbocation.

Alkenes are much stronger bases than alkanes, requiring a much lower acid strength from the zeolite, which makes their adsorption possible by weak acid sites. This means that alkenes can form a carbocation more easily than the alkanes, acting as initiating agents if added in small amounts, but in larger amounts they can poison the zeolite surface, occupying most of the acid sites (330). Finally, there are also authors proposing a radical or ion-radical mechanism for the activation of the alkane (331–334).

Nevertheless, theoretical modeling has proved to be a very useful technique in the study of reaction mechanisms, allowing the scientist to try several alternative mechanisms and avoiding numerous hours spent planning and performing experiments. Using these theoretical models one can plan experiments to verify the veracity of the mechanisms validated by the modelling. Despite the great potential that quantum chemical calculations present, there is still

a lot of work to be done in the development of more accurate and reliable theoretical models.

It is possible to find in the literature several applications of molecular modelling aimed at determining reaction heats and activation energies of well-known reactions, in order to test the accuracy of the theoretical models. Initially, the values obtained through theoretical models differed substantially from the experimental ones, but with application of more complex methods, differences tend to be reduced and theoretical values are becoming more and more reliable.

At first, when large calculations were not possible due to computational limitations, the main simplifications were the low levels of theory and the use of small clusters (usually not bigger than three tetrahedral atoms (3T)) to simulate the acid centre of the zeolite. In 1996, Blaszkowski et al. used a local DFT method with a 3T cluster to study the cracking of ethane and determined an activation barrier of 322 kJ mol^{-1} (325).

Zygmund et al. studied the influence of the surrounding atoms of the acid site, using several clusters with different sizes (5, 18, 28, 38, 46, and 58T atoms models) and DFT methods (335). They also studied cracking of ethane and a 5T cluster and found an activation barrier energy value varying between 211.5 and 226 kJ mol^{-1}, depending on the level of theoretical method used. Depending on the size of the cluster, differences from –31.8 (18T cluster) to –61 kJ mol^{-1} (58T cluster) were obtained.

Experimental values for the activation barrier of ethane are not available in the literature. However, since values measured for n-alkanes from propane to hexane are similar (336), it is realistic to expect the energy for the activation barrier of ethane to be similar to the value of 196 $\pm$ 12 kJ mol^{-1} (336) experimentally obtained for propane.

It is clear that, with the refinement of theoretical methods, the values obtained are getting closer to experimental ones, indicating that theoretical modelling is becoming a very powerful and useful tool in the study of zeolite chemistry and, as this tools become available, the relation between acidity and activity will become clearer. Nevertheless, the objective of determining acidity-activity relationships is at hand and can be developed along the lines that have been used for homogeneous catalysis.

As stated at the beginning of this article, the relationship between acidity and activity has been well established for homogeneous acid catalysis for a long time with the works of Semenov (337) and Polanyi (338) and the use of linear free-energy relationships (339–341) which have been updated by the works of Marcus (342) and Blowers and Masel (343), who proposed different nonlinear relationships between the activation energy for a reaction and its ergonicity.

Although homogeneous acid catalysis has seen advances in this field, heterogeneous catalysis has been a more difficult field, in view of the different aspects we have already covered above. The use of linear free-energy

relationships for heterogeneous catalysis has been addressed by Yoneda in the late 1960s and early 1970s (229,344) but, in fact, attempts to correlate acidity and activity resulted in highly non-linear or non-existent relationships (227,228–347). Worth mentioning is a particular study where Knözinger compares the characterization of zeolite acidity by spectroscopic and catalytic means (226); in the words of the authors ". . . spectroscopic and catalytic observations do not match perfectly for the four zeolite materials that were compared."

The use of quantitative correlations may prove difficult for complex reactions since the mechanisms themselves are very intricate (348).

A recent study on the ethylation of benzene with ethanol over nano-sized HZSM-5 arrived at some correlations that indicate that sites of different strength promote different reactions (349), but these may be only seen as qualitative relationships.

Over the years, however, the situation has evolved and several relationships were obtained. Using an acidity scale based on Hammett's indicators, Hashimoto found a relationship between acidity and activity on silica-aluminas (350).

Using a decomposition methodology, as discussed above, to obtain the acid strength distribution of a catalyst from its ammonia TPD curve, it was found that the activity of ethene, propene, 1-butene, i-butene, and n-heptane transformations could be correlated with the acidity using a linear Brønsted-type relationship and resorting to the activation energy for the desorption of ammonia as an acid strengthscale (106,129,130). In these works, the observed activity was considered to be the summation of the activities of the different acid sites with uniform activation energy for the desorption of ammonia (E^i), weighted by the amount of those sites in the catalyst (q_{E0^i}), thus taking into account both the strength and the number of acid sites:

$$A_c = \sum_i q_{E0^i} \alpha_c \, e^{\beta_c E^i},$$

where α_c and β_c are, respectively, the intrinsic activity (when the activation energy for the desorption of ammonia is zero) and the sensitivity towards the acid strength as measured by that activation energy.

Although the values of α_c and β_c should be mainly dependent on the reaction itself, since the model did not account for structure-related effects, it can also depend on the structure of the catalyst as it imposes restrictions on the geometry of the transition-state and on the possible reaction mechanisms. It was observed that the values of α_c and β_c are constant for a certain reaction inside a family of zeolites. The results obtained from kinetic experiments are summarized in Table 6.

Table 6: α_c and β_c values of Brønsted-type equation for the transformation of light olefins on HNaY and HNaUSY zeolites and for the transformation of n-heptane on MFI and ReY zeolites.

Family of zeolites	Reactant	α_c (mol h^{-1} g^{-1} acid $site^{-1}$)* $\times 10^9$	β_c (mol kJ^{-1}) $\times 10^2$
HNaY(102)	Ethene	0.011	5.0
	Propene	0.23	5.5
	1-Butene	1.1	4.2
	Isobutene	1.8	4.1
Ultra stable HNaY(102)	Ethene	0.7	1.2
	Propene	2.6	1.6
	1-Butene	11	0.53
	Isobutene	9.1	0.8
MFI(85)	n-Heptane	1.32	1.69
ReY(85)	n-Heptane	0.905	3.44

Very recently, this methodology was also applied to the transformation of m-xylene and methylcyclohexane over BEA zeolites (351). This type of relations has already been supported by molecular modelling calculations, using an ab initio HF approximation (269,292,352) and a short review on this subject has been published recently, where the alternatives to Brønsted-type equations, namely the ones proposed by Marcus and by Blowers and Masel, are also discussed (291). Although these studies have relied on the characterization of the acidity of the zeolites by means of ammonia TPD, it was also shown that it is possible to correlate the activity with acidity measurements obtained by pyridine desorption followed by FTIR (353). Inclusion of this type of relationships into more complex kinetic equations has also been attempted with success (290).

A linear relationship between the activation energy for various reactions involved in the conversion of ethane (354) and propane (355) with the deprotonation energy of the site were also reported by Blowers. Ingelsten and co-workers found a good correlation, although only qualitative, between the NO_2 reduction by propane over HZSM-5 and the acidity of the catalyst (356).

This type of findings has been increasing in the recent years and, in 2010, Niwa reported on relationships between the activation energy and the acid strength of the sites, as measured by the heat of adsorption of ammonia, for a series of zeolites on the cracking of hexane and octane and concluded that, for some zeolites, there is a linear decrease in activation energy with the acid strength of the sites but that, for others, this relationship was not observed (357). Niwa has also reported decreasing linear relationships between the activation energy for the cracking of octane (over a series of different zeolites) (358) and hexane (on HZSM-5) (29) and the acid strength of the active sites. However, the latter study shows a different relationship when the activation energy for the cracking of octane is plotted against the acid strength, whereby

the activation energy increases with acid strength for more acidic sites when the reaction is carried-out on HZSM-5 (29).

Very recently, good correlations for the direct synthesis of hydrogen peroxide from hydrogen and oxygen with the Brønsted acidity of ZSM-5 catalysts have also been reported (359); the results presented also emphasized the interaction between the Brønsted and the Lewis acid sites. Another clear correlation that implies the interaction between Brønsted and Lewis acidity is the report by Faro Jr. that the activity for propane aromatization correlates well with the product of the strong Lewis and Brønsted acid site concentrations (360).

There are, however, some quantum chemical calculations that seem to imply that the catalytic effect is related not only to acidity, but also to van der Waals interactions of the reactants with the inner surface of the zeolite pores and cavities; furthermore, the results also seem to be heavily dependent on the quantum model that is used (361). Other studies have also concluded that the intrinsic acidity of some zeolites is similar; Valyon concluded that the order of intrinsic acidity of a series of zeolites follows the order H-ZSM-5 $\approx$ H-mordenite $\approx$ H-β $>$ H-USY $>$ H-Y (362). The same study also states that the site-specific apparent rate constant of the bimolecular hexane transformation parallels the intrinsic acid strength of the samples, although no quantitative correlation is shown. These observations are also in agreement with some suggestions, by Miller, that the acidity of zeolites is all similar and that most of the effects on activity are due to different adsorption interactions (363,364); Miller observed a compensation effect between the pre-exponential factor and the activation energy that is interpreted as revealing the similarity of the acidity of the different zeolites. In fact, a compensation effect has also been observed for different catalysts in the degradation of polyethylene, even when alumina was used, and this was interpreted as the reaction proceeding through the same mechanism (365).

We believe that these aspects will still be under debate for quite some time, since it is obviously very difficult to separate the chemical and the physical adsorption effects and even when adsorbing ammonia, van der Waals interactions will also occur.

7. DISCUSSION AND CONCLUSIONS

Acidity in solids is a someties rather imperfectly defined concept that includes nature, number (density), strength, and environment of acid sites. It is of great benefit for the design of catalysts to have methods enabling the identification of all these factors.

The Hammett acidity function has been probably overextended to the area of solids, as acid sites in solids are quite heterogeneous in nature and strength. Their characterization is more difficult and complex than for liquids. It is clear

that relative ranking of a series of related materials is more readily obtained than absolute acid strength values.

Acid strength of zeolites depends on many factors and, as a result, various methods have been developed for its characterization and it may be important to characterize the acidity by a variety of methods in particular, since different types of Brønsted and Lewis sites, often interacting, must be considered. Most often, a broad and continuous distribution of acid strengths is observed for a given type of material. Induced heterogeneity, i.e., heterogeneity of the acid sites caused by the measurement itself (i.e., when a basic molecule is adsorbed) should be recognized. Lewis sites also provided adjustment of the acid strength by a cooperative interaction with Brønsted sites. In the case of acid zeolites, acidity (in its various aspects) is the main parameter that determines catalytic activity. Therefore, understanding and quantifying the properties of actid sites inside the zeolite is needed if we want to characterize them as catalytic sites and to better comprehend and predict their behavior towards acid-catalyzed reactions.

There is a need to establish an acidity scale that can be used for solid acids and to determine relations existing between physical and chemical properties and zeolite performances, so that we can develop methods to quickly and efficiently predict the behavior and activity of zeolites.

To develop a suitable acidity characterization, there are three main methods.

- The first one aims at evaluating the strength of the hydroxyl O-H bond using spectroscopic techniques (FT-IR, MAS-NMR), or quantum chemical calculations on representative cluster models of Si, Al (or others), O, and H atoms.
- The second one is based on the quantification of the interaction of a basic probe molecule with the acidic sites by physical (calorimetry, TPD) or spectroscopic (IR, MAS-NMR) techniques and quantum chemical calculations or theoretical modeling.
- The third one is the use of catalytic test reactions with variable acid strength requirements, the selectivity of which may also give some indication on the acid site density.

Solid-state NMR, infrared spectroscopy, adsorption, and desorption of probe molecules and use of model reactions are among the most efficient and most used techniques. Solid NMR can be used with two main goals. The first one is to characterize the chemical elements in the zeolite structure (e.g., Si or Al). This allows one to study the presence, type, and location of acid sites inside (and in some cases outside) the framework. On the other hand, by adsorbing probe molecules or chemical reagents (with or without performing a reaction),

it is possible to determine the types of interactions between those molecules and the active sites.

Infrared studies are mainly used to characterize the hydroxyl groups that are responsible for Brønsted acidity. Those commonly generate one or two broad peaks in the region of 3500-3650 cm^{-1}. Another IR technique is based on adsorption of probe molecules such as carbon monoxide, ammonia, or pyridine. The peaks formed during adsorption process and eventually the disappearance of some or part of the hydroxyl groups peaks can reveal the nature of the acid sites (Brønsted or Lewis) or their location (inside small pores or in large cavities, on framework or on extra-framework sites).

Calorimetric and TPD methods allow one to construct an acid site strength Determining adsorption and desorption energies of probe molecules is a useful and powerful tool. The use of appropriate molecules leads to the establishment of a trustful and sensitive scale of acidity, which can be used to compare the acid strength of zeolites amongst themselves. It is even possible to determine the distribution of acid strength of several sites inside a zeolite by decomposing TPD curves or by microcalorimetry of probe molecule adsorption by pulses. Using a Brønsted relation-type equation, modified for acid sites strength distribution, it is possible to predict the activity of a zeolite towards a certain reaction, accounting simultaneously for the influence of all different strengths of active sites.

Although calorimetric and TPD methods allow one to construct an acid site strength distribution "map," there are experimental aspects, such as the dependance of the results on the acid site concentration and heating rate, in addition to acid site strength, that have to be taken into account. The advent of methods enabling the decomposition and quantification of TPD patterns is certainly a major development, as it enables the replacement of a time-consuming static calorimetry technique by a dynamic and fast one. These techniques have also allowed successful correlations between the activity and the acidity, covering different catalysts.

Evaluating the strength of the bridging hydroxyl bond may indeed somewhat reflect the acid strength. However, this approach does not take into account the fact that acid strength is, in practice, relative, since it depends on the nature of the base. For NMR, diamagnetic shifts induced by the presence of the adsorbate or additional paramagnetic shifts resulting from the interaction of the adsorbate with its environment may lead to adsorbate resonance peak shifts that should be interpreted with some caution.

Similar precautions should hold for theoretical evaluations of acid strength, the situation being even more complicated and challenging because of the need to define representative models and to access computing methods and resources to handle large systems. With respect to theoretical and modeling approaches, there is no comment but one: the quality of the response depends on the model and method.

Model reactions constitute an efficient tool not only to check the suitability of solid acids as catalysts, but also to characterize most of the parameters that influence surface acid catalysis (type of acid sites, their strength, and density). However, it is important to emphasize that only sites active in the reaction at hand can be characterized by this technique. Preferably, the reaction chosen for characterizing one element of acidity (strength or site density) should not be sensitive to the others and, in order to correlate the characterization with other catalytic results, the reactions chosen should be of similar nature. As a result, only monomolecular reactions can be used for characterising acid strength. Rate ratio of bimolecular to monomolecular reactions, when they require acid sites of comparable strength, may be used to characterize site density. Confinement effects that determine actual concentration of reactant molecules near the active sites also affect the actual reaction rate. Last but not least, one should also be aware that for acid catalysts the initial deactivation is often rapid and that, consequently, the determination of the true initial activity may be difficult.

Separating and controlling chemical and structural effects affecting the acid strength of zeolites are challenges that have prevented to a large extent the successful quantification of zeolite acid strength and its relation to catalytic activity.

The use of combined techniques (e.g., IR-MS-TPD) allows one to know the distribution of Brønsted and Lewis acid sites as a function of acid strength on the catalytic surface, and how the interaction between those can increase Brønsted acidity.

In a research environment, where appropriate resources are available, the combination of chemical-spectroscopic (infrared and NMR) techniques, coupled with microcalorimetry and TPD of several basic molecules, will most probably provide the information necessary to relate acid strength to catalyst performance for both model or targeted reactions. For monitoring purposes, in a catalyst production environment, where quality control is important, TPD techniques are low cost and most effective.

A significant set of methods that have been developing in recent years — microspectroscopy — is beginning to enable the analysis of phenomena at particle and site level and are likely to gain importance in the near future.

One major aspect in the fundamental understanding of the acid-catalyzed reactions and in creating the ability to predict catalytic behavior from acid strength characterization is the development, in the last decade, of techniques that allow the correlation between the acidity of a catalyst and the activity that is obtained. Although this type of relations has been well established for homogeneous acid catalysis, it has been more difficult to obtain suitable relationships in the case of heterogeneous catalysts due to a variety of problems that have been circumvented in the last years.

The relation between the acidity and the activity, coupled with an increased knowledge on the influence of the structure effects on the reactions, are also needed to power the ability to extrapolate laboratory kinetic reaction data all the way to the industrial application of these reactions — a detailed kinetic model is increasingly more important when designing and tuning industrial reactors.

The relationship between acidity and activity has also gained increasing support from theory. The increase of computational capabilities has allowed for more detailed quantum chemical calculations both on the nature of the acid sites on zeolites and on its action in acid-catalyzed processes. It should be noted, however, that some conclusions can be unequivocally extracted from quantum chemical modelling, including the clear relationship that does exist between the acid strength and the decrease in activation energy for the reactions that take place on these sites. However, quantum chemical modelling still has a long way to go before it can provide definitive answers to more specific questions. In fact, from the literature we can see that the results are still highly dependent on the particular quantum model that is used. Most studies use either Hartree-Fock or DFT calculations, with different basis sets. Nevertheless, semi-empirical and even molecular mechanics methods still have a place in the "computational arsenal" at the disposal of the researcher, in particular in cases where large structures are treated at different quantum-levels, like the ONIOM approaches — the active site is computed with a more accurate theoretical model than the outer layers. In this area, it is noticeable the yet incipient use of quantum methods resorting to advanced correlation, like the Moeller-Plesset methods, despite the high probability that correlation effects play an important role in the catalytic processes involving acid sites.

In conclusion, a variety of methods has been developed, both at the experimental and theoretical level, to analyze and understand the acidity of solids, in particular of zeolites, and to relate that acidity to the catalytic activity that is observed. The combination of all these methods is allowing the development of some insight into the processes involved in solid acid-catalyzed processes and this will enable, in the future, the possibility to predict the catalytic behavior of any catalyst, as well as to assist in the design of new and more efficient materials.

ACKNOWLEDGMENTS

This article was finalized in honor of Eric Derouane and of Fernando Ramôa Ribeiro. Before his unexpected death, Eric Derouane contributed largely to its writing as the subject was one of his major scientific interests dealing with acidity and zeolites. Fernando Ramôa Ribeiro, also departed recently, had a particular interest in this subject as it was one of the most important topics in his group's research.

REFERENCES

[1] Walling, C. *J. Amer. Chem. Soc*. **1950**, *72*, 1164.

[2] Hammett, L.P.; Deyrup, A.J. *J. Amer. Chem. Soc*. **1932**, *54*, 2721.

[3] Zecchina, A.; Lamberti, C.; SBordiga, S. *Catal. Today* **1998**, *41*, 169–177.

[4] Benesi, H.A. *J. Amer. Chem. Soc*. **1956**, *78*, 5490; *J. Phys. Chem*. **1957**, *61*, 970; *J. Catal*. **1973**, *28*, 176.

[5] Benesi, H.A.; Winquist, B.H.C. *Adv. Catal*. **1978**, *27*, 97.

[6] Hirschler, H.; Schneider, A. *J. Chem. Eng. Data* **1961**, *6*, 313.

[7] Moscou, L,; Mone, R. *J. Catal*. **1973**, *30*, 417.

[8] Hammett, L.P. *J. Phys. Chem*. **1940**, *8*, 644.

[9] Deeba, J.; Hall, W.K. *J. Catal*. **1979**, *60*, 417.

[10] Tanabe, K. *Solid Acids and Bases*, Academic Press, New York, 1970.

[11] Chen, N.Y.; Garwood, W.E.; Dwyer, F.G. *Shape Selective Catalysis in Industrial Applications*, Marcel Dekker, New York, 1989.

[12] Degnan, T.F. *J. Catal*. **2003**, *216*, 32.

[13] Corma, A. *J. Catal*. **2003**, *216*, 298.

[14] Derouane, E.G. *J. Mol. Catal. A Chem*. **1998**, *134*, 29.

[15] Barrer, R.M. in *Zeolites: Science and Technology*, Ramôa Ribeiro, F.; Rodrigues, A. Rollmann, D.; Naccache, C., Eds., NATO ASI Series, Martinus Nijhoff, The Hague, E- **1984**, *80*, 227.

[16] Weisz, P.B.; Frilette, V.J. *J. Phys. Chem*. **1960**, *64*, 382.

[17] Weisz, P.B. *Adv. Catal*. **1962**, *13*, 137.

[18] Sherman, J.D. in *Zeolites: Science and Technology*, Ramôa Ribeiro, F.; Rodrigues, A.; Rollmann, D.; Naccache, C., Eds., NATO ASI Series, Martinus Nijhoff, The Hague, E-**1984**, *80*, 583.

[19] Frilette, V.J.; Weisz, P.B. US Patent 3,140,322, assigned to Mobil Oil Co., 1958.

[20] Frilette, V.J.; Weisz, P.B.; Golden, R.L. *J. Catal*. **1962**, *1*, 301.

[21] Planck, C.J.; Rosinsky, E. US Patent 3,140,251, assigned to Mobil Oil Co., 1961.

[22] Frilette, V.J.; Weisz, P.B. US Patent 3,140,252, assigned to Mobil Oil Co., 1961.

[23] Planck, C.J.; Rosinsky, E. *Ind. Eng. Chem. Prod. Res. Dev*. **1964**, *3*, 165.

[24] Chen, N.Y.; Mazuik, J.; Schwartz, A.B.; Weisz, P.B. *Oil and Gas J*. **1968**, *66*, 154.

[25] Schoonheydt, R.A.; Weckhuysen, B.M. *Phys. Chem. Chem. Phys*. **2009**, *11*, 2794.

[26] Bolton, A.P.; Lanewala, M.A. *J. Catal*. **1970**, *18*, 1970.

[27] Lago, R.M.; Haag, W.O.; Mikowsky, R.J.; Olson, D.H.; Hellring, S.D.; Schmitt, K.D.; Kerr, G.T. *Stud. Surf. Sci. Catal*. **1986**, *28*, 677.

[28] Mirodatos, C.; Barthomeuf, D. *J. Chem. Soc. Chem. Commun*. **1981**, 39.

[29] Niwa, M.; Sota, S.; Katada, N. *Catal. Today* **2012**, *185*, 17.

[30] Zahmakiran, M.; Özkar, S. *Langmuir* **2009**, *25*, 2667.

[31] Nassar, N.N.; Hassan, A.; Pereira-Almao, P. *J. Colloid. Interf. Sci*. **2011**, *360*(1), 233.

[32] Satsuma, A.; Yang, D.; Shimizu, K. *Microp. Mesop. Mat*. **2011**, *141*, 20.

[33] Das, S.K.; Kapoor, S.; Yamada, H.; Bhattacharyya, A.J. *Microp. Mesop. Mat*. **2009**, *118*, 267.

[34] Bisio, C.; Martra, G.; Coluccia, S.; Massiani, P. *J. Phys. Chem. C* **2008**, *112*, 10520.

[35] Suzuki, K.; Katada, N.; Niwa, M. *J. Phys. Chem. C* **2007**, *111*, 894.

[36] Rabo, J.A.; Gajda, G.J. in *Guidelines for Mastering the Properties of Molecular Sieves*, Barthomeuf, D.; Derouane, E.G.; Hoelderich, W.; Eds., NATO ASI Series, Plenum Press, New York, **1990**, *B-221*, 273.

[37] Barthomeuf, D. *Mater. Chem. Phys*. **1987**, *17*, 49.

[38] Ungureanu, A.; Dragoi, B.; Hulea, V.; Cacciaguerra, T.; Meloni, D.; Solinas, V.; Dumitriu, E. *Microp. Mesop. Mater*. **2012**, *163*, 51.

[39] Derouane, E.G.; Chang, C.D. *Microp. Mesop. Mater*. **2000**, *35–36*, 425.

[40] Du, H.; Olson, D.H. *J. Phys. Chem. B* **2002**, *106*, 395.

[41] Barrer, R.M. *J. Chem. Soc*. **1950**, 2342.

[42] Weisz, P.B.; Frilette, V.J.; Maatman, R.W.; Mower, R.W. *J. Catal*. **1962**, *1*, 307.

[43] Haag, W.O.; Dessau, R.M. in *Proceedings 8th Intern. Congress on Catalysis*, Berlin, Dechema, Frankfurt am Main, **1984**, *2*, 305.

[44] Haag, W.O.; Dessau, R.M.; Lago, R.M. *Stud. Surf. Sci. Catal*. **1991**, *60*, 255.

[45] Pellet, R.J.; Blackwell, C.S.; Rabo, J.A. *J. Catal*. **1988**, *114*, 71.

[46] Dwyer, J. in *Guidelines for Mastering the Properties of Molecular Sieves*, Barthomeuf, D.; Derouane, E.G.; Hoelderich, W., Eds., NATO ASI Series, Plenum Press, New York, **1990**, *B-221*, 241.

[47] Segal, E.; Ivanova, I.; Derouane, E.G. *Rev. Roum. Chim*. **1993**, *38*, 1127.

[48] Martens, J.A.; Souverijns, W.; van Rhyn, W.; Jacobs, P.A. in *Handbook of Heterogeneous Catalysis*, Knözinger, H. et al., Ed., Wiley-VCH, Weinheim, **1997**, *1*, 324.

[49] Wang, Y.; Zhou, D.; Yang, G.; Miao, S.; Liu, X.; Bao, X. *J. Phys. Chem. A* **2004**, *108*, 6730.

[50] Khabtou, S.; Chevreau, T.; Lavalley, J.C. *Microp. Mesop. Mater*. **1994**, *3*, 133.

[51] Li, S.; Zheng, A.; Su, Y.; Zhang, H.; Chen, L.; Yang, J.; Ye, C., Deng, F. *J. Amer. Chem. Soc*. **2007**, *129*, 11161.

[52] Katada, N.; Suzuki, K.; Noda, T.; Sastre, G.; Niwa, M. *J. Phys. Chem. C* **2009**, *113*, 19208.

[53] Rabo, J.A. in *Zeolite Chemistry and Catalysis*, Rabo, J.A., Ed., American Chemical Society, Washington, **1976**, 332.

[54] Rabo, J.A. *Catal. Rev. Sci. Eng*. **1981**, *23*, 293.

[55] Noller, H.; Klading, W. *Catal. Rev. Sci. Eng*. **1976**, *13*, 149.

[56] Barthomeuf, D. *J. Phys. Chem*. **1979**, *83*, 249.

[57] Barthomeuf, D. *Stud. Surf. Sci. Catal*. **1980**, *5*, 55.

[58] Mortier, W.J. *Stud. Surf. Sci. Catal*. **1986**, *28*, 423.

[59] Mortier, W.J. *Stud. Surf. Sci. Catal*. **1988**, *37*, 253.

[60] Derouane, E.G.; André, J.M.; Lucas, A.A. *J. Catal*. **1988**, *110*, 58.

[61] Derouane, E.G. in *Guidelines for Mastering the Properties of Molecular Sieves*, Barthomeuf, D., Derouane, E.G.; Hoelderich, W., Eds., NATO ASI Series, Plenum Press, New York, **1990**, *B-221*, 225.

[62] Sastre, G.; Corma, A. *J. Mol. Catal. A Chem*. **2009**, *305*, 3.

[63] Denayer, J.F.M.; Devriese, L.I.; Couck, S.; Martens, J.; Singh, R.; Webley, P.A.; Baron, G.V. *J. Phys. Chem. C* **2008**, *112*, 16593.

[64] Corma, A.; García, H.; Sastre, G.; Viruela, P.M. *J. Phys. Chem. B* **1997**, *101*, 4575.

[65] Simon-Masseron, A.; Marques, J.P.; Lopes, J.M.; Ramôa Ribeiro, F.; Gener, I.; Guisnet, M. *Appl. Catal. A Gen*. **2007**, *316*, 75.

[66] Louis, B.; Vicente, A.; Fernandez, C.; Valtchev, V. *J. Phys. Chem. C* **2011**, *115*, 18603.

[67] Védrine, J.C. in *Guidelines for Mastering the Properties of Molecular Sieves*, Barthomeuf, D.; Derouane, E.G.; Hölderich, W., Eds., NATO ASI Series, Plenum Press, New York, **1990**, *B-221*, 121.

[68] Auroux, A. *Mol. Sieves* **2008**, *6*, 45.

[69] Hunger, M. in *Zeolites and Catalysis, Synthesis Reactions and Applications*, Cejka, J.; Corma, A.; Zones, S., Eds., Wiley-VCH, Wheinheim, **2010**, *2*, 105.

[70] Busco, C.; Barbaglia, A.; Broyer, M.; Bolis, V.; Foddanu, G.M.; Ujliengo, P. *Therm. Acta* **2004**, *418*, 3.

[71] Auroux, A. *Top. Catal*. **2002**, *19*, 205.

[72] Cardona-Martínez, N.; Dumesic, J.A. *J. Catal*. **1990**, *125*, 427.

[73] Mekki-Barrada, A.; Aurroux, A. Thermal Methods, in *Characterization of Solid Materials and Heterogeneous Catalysts, From Structure to Surface Reactivity*, Che, M.; Védrine, J.C., Eds., Wiley-VCH, Weinheim, **2012,** 747.

[74] Chronister, C.W.; Drago, R.S. *J. Amer. Chem. Soc*. **1993**, *115*, 4793.

[75] Drago, R.S. *Applications of Electrostatic-Covalent Models in Chemistry*, Surfside Scientific Publ., Gainesville, Florida, **1994**, 269.

[76] Dias, J.A.; Osegovic, J.P.; Drago, R.S. *J. Catal*. **1999**, *183*, 83.

[77] Dias, S.C.L.; Macedo, J.L.; Dias, J.A. *Phys. Chem. Chem. Phys*. **2003**, *5*, 5574.

[78] Macedo, J.L.; Dias, S.C.L.; Dias, J.A. *Microp. Mesop. Mater*. **2004**, *72*, 119.

[79] Ghesti, G.F.; de Macedo, J.L.; Parent, V.C.I.; Dias, J.A.; Dias, S.C.L.; *Microp. Mesop. Mater*. **2007**, *100*, 27.

[80] de Macedo, J.L.; Ghesti, G.F.; Dias, J.A.; Dias, S.C.L. *Phys. Chem. Chem. Phys*. **2008**, *10*, 1584.

[81] Rodríguez-González, L.; Hermes, F.; Bertmer, M.; Rodríguez-Castellón, E.; Jiménez-López, A.; Simon, U. *Appl. Catal. A Gen*. **2007**, *328*, 174.

[82] Auroux, A.; Jin, Y.S.; Védrine, J.C. *Appl. Catal*. **1988**, *36*, 323.

[83] Hunger, A.; Szombathely, M.V. *Z. Phys. Chem*. **1995**, *190*, 19.

[84] Cvetanovic, R.J.; Amenomiya, Y. *Adv. Catal*. **1967**, *17*, 103.

[85] Karge, H.G.; Dondur, V.; Weitkamp, J. *J. Phys. Chem*. **1991**, *95*, 283.

[86] Ison, A.; Gorte, R.J. *J. Catal*. **1984**, *89*, 150.

[87] Costa, C.; Lopes, J.M.; Lemos, F.; Ramôa Ribeiro, F. *J. Mol. Catal. A Chem*. **1999**, *144*, 221.

[88] Niwa, M.; Suzuki, K.; Katada, N.; Kanougi, T.; Atoguchi, T. *J. Phys. Chem. B* **2005**, *109*, 18749.

[89] Rodríguez-González, L.; Simon, U. *Meas. Sci. Technol*. **2010**, *21*, 027003

[90] Cvetanovic, R.J.; Amenomiya, Y. *Catal. Rev*. **1972**, *10*, 21.

[91] Sawa, M.; Niwa, M.; Murakami, Y. *Zeolite* **1990**, *10*, 307.

[92] Joly, J.P.; Perrard, A. *Langmuir* **2001**, *17*, 1538.

[93] Hashimoto, K.; Masudo, T.; Mori, T. *Stud. Surf. Sci. Catal*. **1986**, *28*, 503.

[94] Forni, L.; Magni, E. *J. Catal*. **1988**, *112*, 437.

[95] Forni, L.; Magni, E.; Ortoleva, E.; Monaci, R.; Solinas, V. *J. Catal*. **1988**, *112*, 444.

[96] Karge, H.G.; Dondur, V. *J. Phys. Chem*. **1990**, *94*, 765.

[97] Niwa, M.; Katada, N.; Masahiko, M.; Murakami, Y. *J. Phys. Chem*. **1995**, *99*, 8812.

[98] Hunger, B.; Szombathely, M.V.; Hoffmann, J.; Brauner, P. *J. Therm. Anal*. **1995**, *44*, 293.

[99] Delgado, J.; Goméz, J. *Langmuir* **2005**, *21*, 3503.

[100] Gorte, R. *J. Catal*. **1982**, *75*, 164.

[101] Delgado, J.; Goméz, J. *Langmuir* **2005**, *21*, 9555.

[102] Katada, N.; Igi, H.; Kim, J.-H.; Niwa, M. *J. Phys. Chem. B* **1997**, *101*, 5969.

[103] Martin, A.; Wolf, U.; Berndt, H.; Lucke, B. *Zeolites* **1993**, *13*, 309.

[104] Robb, G.M.; Zhang, W.; Smirniotis, P.G. *Microp. Mesop. Mater*. **1998**, *20*, 307.

[105] Auroux, A.; Vedrine, J.C. *Stud. Surf. Sci. Catal*. **1985**, *20*, 311.

[106] Costa, C.; Dzikh, I.P.; Lopes, J.M.; Lemos, F.; Ramôa Ribeiro, F. *J. Mol. Catal. A* Chem. **2000**, *154*, 193.

[107] Miyamoto, Y.; Katada, N.; Niwa, M. *Microp. Mesop. Mater*. **2000**, *40*, 271.

[108] Katada, N.; Miyamoto, Y.; Begum, H.; Naito, N.; Niwa, M.; Matsumoto, A.; Tsutsumi, K. *J. Phys. Chem. B* **2000**, *104*, 5511.

[109] Barrie, P. *Phys. Chem. Chem. Phys*. **2008**, *10*, 1688.

[110] Jaroniec, M.; Sokołowski, S.; Cerofolini, G.F. *Thin Solid Films* **1976**, *31*, 321.

[111] Jaroniec, M.; Borówko, M. *J. Colloid Interf. Sci*. **1978**, *63*, 362.

[112] Hsu, C.C.; Wojciechowski, B.W.; Rudzinski, W.; Narkiewicz, J. *J. Colloid Interf. Sci*. **1978**, *67*, 292.

[113] Rudzinski, W.; Borowiecki, T.; Panczyk, T.; Dominko, A. *Adv. Colloid Interf. Sci*. **2000**, *84*, 1.

[114] Rudzinski, W.; Panczyk, T.; Plazinski, W. *J. Phys. Chem. B* **2005**, *109*, 21868.

[115] Chen, D.T.; Sharma, S.B.; Filimonov, I.; Dumesic, J.A. *Catal. Lett*. **1992**, *12*, 201.

[116] Garrone, E.; Fubini, B.; Bonelli, B.; Onida, B.; Otero Areán, C. *Phys. Chem. Chem. Phys*. **1999**, *1*, 513.

[117] Egerton, T.A.; Stone, F.S. *Trans. Faraday Soc*. **1970**, *66*, 2364.

[118] Strunk, J.; Naumann d'Alnoncourt, R.; Bergmann, M.; Litvinov, S.; Xia, X.; Hinrichsen, O.; Muhler, M. *Phys. Chem. Chem. Phys*. **2006**, *8*, 1556.

[119] Esquivel, D.; Cruz-Cabeza, A.J.; Jiménez-Sanchidrián, C.; Romero-Salguero, F.J. *Microp. Mesop. Mater*. **2011**, *142*, 672.

[120] Niwa, M.; Nishikawa, S.; Katada, N. *Microp. Mesop. Mater*. **2005**, *82*, 105.

[121] Suzuki, K.; Noda, T.; Katada, N.; Niwa, M. *J. Catal*. **2007**, *250*, 151.

[122] Noda, T.; Suzuki, K.; Katada, N.; Niwa, M. *J. Catal*. **2008**, *259*, 203.

[123] Suzuki, K.; Aoyagi, Y.; Katada, N.; Choi, M.; Ryoo, R.; Niwa, M. *Catal. Today* **2008**, *132*, 38.

[124] Ramos Pinto, R.; Borges, P.; Lemos, M.A.N.D.A.; Lemos, F.; Védrine, J.C.; Derouane, E.G.; Ramôa Ribeiro, F. *Appl. Catal. A Gen*. **2005**, *284*, 39.

[125] Shannon, R.D.; Gardner, K.H.; Staley, R.H.; Bergeret, G.; Gallezot, P.; Auroux, A. *J. Phys. Chem*. **1985**, *89*, 4778.

[126] Borges, P.; Ramos Pinto, R.; Lemos, M.A.N.D.A.; Lemos, F.; Védrine, J.C.; Derouane, E.G.; Ramôa Ribeiro, F. *Appl. Catal. A Gen*. **2007**, *324*, 20.

[127] Costa, L.; Coelho, A.; Lemos, F.; Ramôa Ribeiro, F.; Cabral, J.M.S. *Appl. Catal. A Gen*. **2009**, *354*, 33.

[128] Coelho, A.; Costa, L.; Marques, M.M.; Fonseca, I.M.; Lemos, M.A.N.D.A.; Lemos, F. *Appl. Catal. A* **2012**, *413–414*, 183.

[129] Costa, C.; Lopes, J.M.; Lemos, F.; Ramôa Ribeiro, F. *J. Mol. Catal. A Chem*. **1999**, *144*, 233.

[130] Costa, C.; Lopes, J.M.; Lemos, F.; Ramôa Ribeiro, F. *Catal. Lett*. **1997**, *44*, 255.

[131] Penzien, J.; Abraham, A.; van Bokhoven, J.A.; Jentys, A.; Muller, T.E.; Sievers, C.; Lercher, J.A. *J. Phys. Chem. B* **2004**, *108*, 4116.

[132] Wang, B.; Manos, G. *Ind. Eng. Chem. Res*. **2007**, *46*, 7977.

[133] Lercher, J.A.; Gründling, C.; Eder-Mirth, G. *Catal. Today* **1996**, *27*, 353.

[134] Lercher, J.A.; Veefkind, V.; Fajerwerg, K. *Vibr. Spectrosc*. **1999**, *19*, 107.

[135] Ryczkowski, J. *Catal. Today* **2001**, *68*, 263.

[136] Thibault-Starzyk, F. Introduction a l'étude des zéolithes par spectroscopie infrarouge, in *Les Matériaux Micro et Mésoporeux: Caractérisation*, Thibault-Starzyk, F., Ed., EDP Sci. Edit. Paris, **2004**.

[137] Lercher, J.A.; Jentys, A. Infrared and Raman Spectroscopy for Characterizing Zeolites, in *Introduction to Zeolite Science and Practice*, 3rd ed., van Bekkum, H.; Čejka, J.; Corma, A.; Schüth, F., Eds., Elsevier, Amsterdam, **2007**, Ch. 13.

[138] Günzler, H. *IR Spectroscopy*, Wiley-VCH, Weinheim, **2002**.

[139] Haw, J.F. *In Situ Spectroscopy in Heterogeneous Catalysis*, Wiley-VCH, Weinheim, **2002**.

[140] Weitkamp, J.; Puppe, L., Eds., *Catalysis and Zeolites: Fundamentals and Applications*, Springer, Berlin, **1999**.

[141] Kustov, L.M. *Top. Catal*. **1997**, *4*, 131.

[142] Aufdembrink, B.A.; Dee, D.P.; McDaniel, P.L.; Mebrahtu, T.; Slager, T.L. *J. Phys. Chem. B* **2003**, *107*, 10025.

[143] Bevilacqua, M.; Meloni, D.; Sini, F.; Monaci, R.; Montanari, T.; Busca, G. *J. Phys. Chem. C* **2008**, *112*, 9023.

[144] Montanari, T.; Finocchio, E.; Busca, G. *J. Phys. Chem. C* **2011**, *115*, 937.

[145] Mortier, W.J. *J. Catal*. **1978**, *55*, 138.

[146] Jacobs, P.A.; Mortier, W.J.; Uytterhoeven, J.B. *J. Inorg. Nucl. Chem*. **1978**, *40*, 1919.

[147] Jacobs, P.A. *Catal. Rev. Sci. Eng*. **1982**, *24*, 415.

[148] Jacobs, P.A.; Mortier, W.J. *Zeolites* **1982**, *2*, 226.

[149] Sanderson, R.T. *Chemical Bonds and Bond Energy*, 2nd ed., Academic Press, New York, **1976**, 75.

[150] Knözinger, H.; Huber, S. *J. Chem. Soc. Faraday Trans*. **1998**, *94*, 2047.

[151] Ghiotti, G.; Garrone, E.; Morterra, C.; Boccuzzi, F. *J. Phys. Chem*. **1979**, *83*, 2863.

[152] Beebe, T.P.; Gelin, P.; Yates, J.T. *Surf. Sci*. **1984**, *148*, 526

[153] Paukshtis, E.A.; Soltanov, R.I.; Yurchenko, E.N. *React. Kinet. Catal. Lett*. **1982**, *19*, 105.

[154] Izaki, M.I.; Knözinger, H. *Mater. Chem. Phys*. **1987**, *17*, 201.

[155] Morterra, C.; Cerrato, G.; Emanuel, C.; Bolis, V. *J. Catal*. **1993**, *142*, 349.

[156] Maache, M.; Janin, A.; Lavalley, J.C.; Joly, J.F.; Benazzi, E. *Zeolites* **1993**, *13*, 419.

[157] Chakarova, K.; Hadjiivanov, K. *Chem. Commun*. **2011**, *47*, 1878.

[158] Parry, E.P. *J. Catal*. **1963**, *2*, 371.

[159] Lenfrancois, M.; Malbois, G. *J. Catal*. **1971**, *20*, 350.

[160] Hughes, T.R.; White, H.M. *J. Phys. Chem*. **1967**, *71*, 2112.

[161] Datka, J.; Turek, A.M.; Jehng, J.M.; Wachs, I.E. *J. Catal*. **1992**, *135*, 186.

[162] Emeis, C.A. *J. Catal*. **1993**, *141*, 347.

[163] Pelmenshchikov, A.G.; Paukshtis, E.A.; Stepanov, V.G.; Pavlov, V.I.; Yurchenko, E.N.; Ione, K.G.; Beran, S. *J. Phys. Chem*. **1989**, *93*, 6725.

[164] Kubelková, L.; Beran, S.; Malecka, A. Mastikhin, V.M. *Zeolites* **1989**, *9*, 12.

[165] Uytterhoeven, J.W.; Jacobs, P.A.; Makay, K.; Schoonheydt, R. *J. Phys. Chem*. **1968**, *72*, 1768.

[166] Turkevich, J.; Stevenson, P.C. *J. Phys. Chem*. **1943**, *11*, 328.

[167] Kline, C.H.; Turkevich, J. *J. Phys. Chem*. **1944**, *12*, 300.

[168] Basila, M.R.; Kantner, T.R.; Rhee, K.H. *J. Phys. Chem*. **1964**, *68*, 3197.

[169] Ward, J.W. in *Zeolite Chemistry and Catalysis*, Rabo, J.A., Ed., *Amer. Chem. Soc*. Monograph, Washington, **1976**, *171*, 118.

[170] Defosse, C.; Cannesson, P.; Delmon, B. *J. Phys. Chem*. **1976**, *80*, 1028.

[171] Thibault-Starzyk, F.; Travert, A.; Saussey, J.; Lavalley, J.-C. Top. Catal. **1998**, *6*, 111.

[172] Thibault-Starzyk, F.; Gil, B.; Aiello, S.; Chevreau, T.; Gilson, J.-P. *Microp. Mesop. Mater*. **2004**, *67*, 107.

[173] Smirnov, K.S.; Thibault-Starzyk, F. *J. Phys. Chem. B* **1999**, *103*, 8595.

[174] Gil, B.; Košová, G.; Cejka, J. *Microp. Mesop. Mat*. **2010**, *129*, 256.

[175] (a) Jacobs, P.A.; Heylen, C.F. *J. Catal*. **1974**, *34*, 267–274.; (b) Lahousse, C.; Aboulayt, A.; Maugé, F.; Lavalley, J.C. *J. Mol. Catal*. **1993**, *84*, 283–297.

[176] Thibault-Strarzyk, F.; Maugé, F. Infrared Spectroscopy, in *Characterization of Solid Materials and Heterogeneous Catalysts: From Structure to Surface Reactivity*, Che, M.; Védrine, J.C., Eds., Wiley-VCH, Weinheim, **2012**, 3.

[177] Brodskii, I.A.; Zhdanov, S.P. *Proceedings 5th Int Zeolite Conference*, Heyden, London, **1980**, 234.

[178] Ozin, G.A.; Baker, M.D.; Godber, J.; Gil, G.J. *J. Phys. Chem*. **1989**, *93*, 2899.

[179] Baker, M.D.; Ozin, G.A.; Godber, J. *Catal. Rev. Sci. Eng*. **1985**, *27*, 591.

[180] Esemann, H.; Foerster, H.; *Z. Phys. Chem*. **1995**, *189*, 263.

[181] Krause, K.; Geidel, E.; Kindler, J.; Foerster, H.; Smirnow, K.S. *Vib. Spectrosc.* **1996**, *12*, 45.

[182] Drochner, A.; Fehlings, M.; Krauß, K.; Vogel, H. *Chem. Eng. Technol*. **2000**, *23*, 319.

[183] Kotrel, S.; Michael, P.R.; Lunsford, H.J. *J. Catal*. **2000**, *191*, 55.

[184] Kazansky, V.B.; Serykh, A.I.; Semmer-Herledan, V.; Fraissard, J. *Phys. Chem. Chem. Phys*. **2003**, *5*, 966.

[185] Gilson, J.P.; Fernandez, C.; Thibault-Starzyk, F. *J. Mol Catal. A Chem*. **2009**, *305*, 54.

[186] Thomas, J.; Klinowski, J. *Adv. Catal*. **1985**, *33*, 199.

[187] Pfeifer, H.; Freude, D.; Hunger, M. *Zeolites* **1985**, *5*, 274.

[188] Nagy, J.; Derouane, E. *ACS Symp. Ser*. **1988**, *368*, 2.

[189] Stöcker, M. *Adv. Zeolite Sci. App. Stud. Surf. Sci. Catal*. **1994**, *85*, 429.

[190] Hunger, M. *Catal. Rev. Sci. Eng*. **1997**, *39*(4), 345.

[191] Hunger, M. *Microp. Mesop. Mater*. **2005**, *82*, 241.

[192] Ashbrook, S.E.; Smith, M.E. *Chem. Soc. Rev*. **2006**, *35*, 718.

[193] Dybowski, C.; Bai, S. *Anal. Chem*. **2006**, *78*, 3852.

[194] Batamack, P.; Doremieux-Morin, C.; Vincent, R.; Fraissard, J. *Chem. Phys. Lett*. **1991**, *180*, 545.

[195] Heeribout, L.; Dorémieux-Morin, C.; Nogier, J.P.; Vincent, R.; Fraissard, J. *Microp. Mesop. Mater*. **1998**, *24*, 101.

[196] Heeribout, L.; Semmer, V.; Batamack, P.; Dorémieux-Morin, C.; Fraissard, J. *Microp. Mesop. Mater*. **1998**, *21*, 565.

[197] Heeribout, L.; Batamack, P.; Dorémieux-Morin, C.; Vincent, R.; Fraissard, J. *Colloids Surf. A* **1996**, *115*, 229.

[198] Gabelica, Z.; Nagy, J.B.; Bodart, P.; Debras, G.; Derouane, E.G.; Jacobs, P.A. in *Zeolites: Science and Technology,* Ramôa Ribeiro, F.; Rodrigues, A.; Rollmann, D.; Naccache, C., Eds., NATO ASI Series, Martinus Nijhoff, the Hague, E- 80, 1984, 193.

[199] Hajjar, R.; Millot, Y.; Man, P.P.; Che, M; Dzwigaj, S. *J. Phys. Chem. C* **2008**, *112*, 20167.

[200] Xu, B.; Bordiga, S.; Prins, R.; van-Bokhoven, J.A. *Appl. Catal. A Gen*. **2008**, *333*, 245.

[201] Aguado, J.; Serrano, D.P.; Rodríguez, J.M. *Microp. Mesop. Mater*. **2008**, *15*, 504.

[202] Kao, H.M.; Changa, P.C.; Liao, Y.W.; Lee, L.P.; Chien, C.H. *Microp*. *Mesop*. *Mater*. **2008**, *114*, 352.

[203] Beers, E.W.; van Bokhoven, J.A.; de Lathoudera, K.M.; Kapteijna, F.; Moulijn, J.A. *J. Catal*. **2003**, *218*, 239.

[204] Oumia, Y.; Nemotoa, S.; Nawatab, S.; Fukushimab, T.; Teranishia, T.; Sano, T. *Mater. Chem. Phys*. **2002**, *78*, 551.

[205] Pérez-Pariente, J.; Sanz, J.; Fornés, V.; Corma, A. *J. Catal*. **1990**, *124*, 217.

[206] Peng, L.; Huo, H.; Gan, Z.; Grey, C.P. *Microp. Mesop. Mater*. **2008**, *109*, 156.

[207] Peng, L.; Huo, H.; Liu, Y. Grey, C.P. *J. Amer. Chem. Soc*. **2007**, *129*, 335.

[208] Peng, L.; Liu, Y.; Kim, N.; Readman, J.E.; Grey, C.P. *Nat. Mater*. **2005**, *4*, 216.

[209] Readman, J.E.; Kim, N.; Ziliox, M.; Grey, C.P. *Chem. Commun*. **2002**, *23*, 2808.

[210] Bull, L.M.; Cheetham, A.K.; Anupold, T.; Reinhold, A.; Samoson, A.; Sauer, J.; Bussemer, B.; Lee, Y.; Gann, S.; Shore, J.; Pines, A.; Dupree, R. *J. Amer. Chem. Soc*. **1998**, *120*, 3510.

[211] Kanellopoulos, J.; Gottert, C.; Schneider, D.; Knorr, B.; Prager, D.; Ernst, H.; Freude, D. *J. Catal*. **2008**, *255*, 68.

[212] Yan, Z.; Ma, D.; Zhuang, J.; Liu, X.; Liu, X.; Han, X.; Bao, X.; Chang, F.; Xu, L.; Liu, Z. *J. Mol. Catal A Chem*. **2003**, *194*, 153.

[213] Müller, M.; Harvey, G.; Prins, R. *Microp. Mesop. Mater*. **2000**, *34*, 135.

[214] Engelhardt, G.; Jerschkewitz, H.-G.; Sarv, P.; Samoson, A.; Lippmaa, E. *Zeolites* **1987**, *7*, 289.

[215] Maier, S.M.; Jentys, A.; Lercher, J.A. *J. Phys. Chem. C* **2011**, *115*, 8005.

[216] Rabo, J.A.; Gadja, G.J. in *Guidelines for Mastering the Properties of Molecular Sieves*, Barthomeuf, D.; Derouane, E.G.; Hölderich, W., Eds., NATO ASI Series, Plenum Press, New York, B-221, **1990**, 273.

[217] Kao, H.M.; Chang, P.C.; Liao, Y.W.; Lee, L.P.; Chien, C.H. *Microp. Mesop. Mater*. **2008**, *114*, 352.

[218] Peng, L.; Chupas, P.J.; Grey, C.P. *J. Amer. Chem. Soc*. **2004**, *126*, 12254.

[219] Li, S.; Huang, S.-J.; Shen, W.; Zhang, H.; Fang, H.; Zheng, A.; Liu, S.-B.; Deng, F. *J. Phys. Chem. C* **2008**, *112*, 14486.

[220] Fărcaşiu, D.; Ghenciu, A. *Progr. NMR Spectrosc*. **1996**, *29*, 129.

[221] Yu, Z.; Wang, Q.; Chen Lei, L.; Deng, F. *Chin*. *J. Catal*. **2012**, *33*, 129.

[222] Huo, H.; Peng, L.; Grey, C.P. *J. Phys. Chem. C* **2009**, *113*, 8211.

[223] Wang, X.; Coleman, J.; Jia, X.; White, J.L. *J. Phys. Chem. B* **2002**, *106*, 4941.

[224] Wang, W.; Hunger, M. *Acc. Chem. Res*. **2008**, *41*, 895.

[225] Blasco, T. *Chem. Soc. Rev*. **2010**, *39*, 4685.

[226] Kotrel, S.; Lunsford, J.H.; Knözinger, H. *J. Phys. Chem. B* **2001**, *105*, 3917.

[227] Bourdillon, G.; Gueguen, C; Guisnet, M. *Appl. Catal*. **1990**, *61*, 23.

[228] Guisnet, M. *Acc. Chem. Res*. **1990**, *23*, 392.

[229] Yoneda, Y. *J. Catal*. **1967**, *9*, 51.

[230] Kramer, G.; McVicker, G.; Ziemiak, J. *J. Catal*. **1985**, *92*, 355.

[231] McVicker, G.B.; Feeley, O.C.; Ziemiak, J.J.; Vaughan, D.E.W.; Strohmaier, K.C.; Kliewer, W.R.; Leta, D.P. *J. Phys. Chem. B* **2005**, *109*, 2222.

[232] Bilgiç, C.; Tümsek, F. *J. Chromatogr. A* **2007**, *1162*, 83.

[233] Stavitski, E.; Kox, M.H.F.; Weckhuysen, B.M. *Stud. Surf. Sci. Catal*. **2008**, *174*, 21.

[234] Mores, D.; Stavitski, E.; Verkleij, S.P.; Lombard, A.; Cabiac, A.; Rouleau, L.; Patarin, J.; Simon-Masseron, A.; Weckhuysen, B.M. *Phys. Chem. Chem. Phys*. **2011**, *13*, 15985.

[235] Buurmans, I.L.C.; Ruiz-Martínez, J.; van Leeuwen, S.L.; van der Beek, D.; Bergwerff, J.A.; Knowles, W.V.; Vogt, E.T.C.; Weckhuysen, B.M. *Chem. Eur. J*. **2012**, *18*, 1094.

[236] Stavitski, E.; Pidko, E.A.; Kox, M.H.F.; Hensen, E.J.M.; van Santen, R.A.; Weckhuysen, B.M. *Chem. Eur. J*. **2010**, *16*, 9340.

[237] Aramburo, L.R.; Wirick, S.; Miedema, P.S.; Buurmans, I.L.C.; de Groota, F.M.F.; Weckhuysen, B.M. *Phys. Chem. Chem. Phys*. **2012**, *14*, 6967.

[238] Karreman, M.A.; Buurmans, I.L.C.; Geus, J.W.; Agronskaia, A.V.; Ruiz-Martínez, J.; Gerritsen, H.C.; Weckhuysen, B.M. *Angew. Chem. Int. Ed*. **2012**, *51*, 1428.

[239] Kahle, I.; Spange, S. *J. Phys. Chem. C*. **2010**, *114*, 15448.

[240] Campbell, B.J.; Cheetham, A.K.; Vogt, T.; Carluccio, L.; Parker, Jr., W.O.; Flego, C.; Millini, R. *J. Phys. Chem. B* **2001**, *105*, 1947.

[241] Aramburo, L.R.; Karwacki, L.; Cubillas, P.; Asahina, S.; Matthijs de Winter, D.A.; Drury, M.R.; Buurmans, I.L.C.; Stavitski, E.; Mores, D.; Daturi, M.; Bazin, P.; Dumas, P.; Thibault-Starzyk, F.; Post, J.A.; Anderson, M.W.; Terasaki, O.; Weckhuysen, B.M. *Chem. Eur. J*. **2011**, *17*, 13773.

[242] López, N.; Almora-Barrios, N.; Carchini, G.; Blonski, P.; Bellarosa, L.; García-Muelas, R.; Novell-Leruth, G.; García-Mota, M. *Catal. Sci. Technol*. **2012**, *2*, 2405.

[243] Yang, C.-S.; Mora-Fonz, J.M.; Catlow, C.R.A. *J. Phys. Chem. C* **2012**, *116*, 22121.

[244] van Santen, R.A. *Catal. Today* **1997**, *38*, 377.

[245] Sauer, J.; Ugliengo, P.; Garrone, E.; Saunders, V.R. *Chem. Rev*. **1994**, *94*, 2095.

[246] Moore, E.A. *Ann. Rep. Prog. Chem. Sect. A Inorg. Chem*. **2012**, *108*, 449.

[247] Boscoboinik, J.A.; Yu, X.; Yang, B.; Fischer, F.D.; Włodarczyk, R.; Sierka, M.; Shaikhutdinov, S.; Sauer, J.; Freund, H.-J. *Angew. Chem. Int. Ed*. **2012**, *51*, 6005.

[248] Göltl, F.; Grüneis, A.; Bučko, T.; Hafner, J. *J. Chem. Phys*. **2012**, *137*, 114111.

[249] Suzuki, K.; Noda, T.; Sastre, G.; Katada, N.; Niwa, M. *J. Phys. Chem. C* **2009**, *113*, 5672.

[250] Stoyanov, S.R.; Gusarov, S.; Kuznicki, S.M.; Kovalenko, A. *J. Phys. Chem. C* **2008**, *112*, 6794.

[251] Barone, G.; Casella, G.; Giuffrida, S.; Duca, D. *J. Phys. Chem. C* **2007**, *111*, 13033.

[252] Li, Y.; Guo, W.; Fan, W.; Yuan, S.; Li, J.; Wang, J.; Jiao, H.; Tatsumi, T. *J. Mol. Catal. A Chem*. **2011**, *338*, 24.

[253] Wang, N.; Zhang, M.; Yu, Y. *Microp. Mesop. Mat*. **2013**, *169*, 47.

[254] Grajciar, L.; Areán, C.O.; Pulido, A.; Nachtigall, P. *Phys. Chem. Chem. Phys*. **2010**, *12*, 1497.

[255] Grajciar, L.; Areán, C.O.; Pulido, A.; Nachtigall, P. *Phys. Chem. Chem. Phys*. **2010**, *12*, 1497.

[256] Mota, C.J.A.; Bhering, D.L.; Rosenbach, Jr, N. *Angew. Chem. Int. Ed*. **2004**, *43*, 3050.

[257] Rosenbach, Jr., N.; Mota, C.J.A. *Appl. Catal. A Gen*. **2008**, *336*, 54.

[258] Agarwal, V.; Huber, G.W.; Conner, Jr., W.C.; Auerbach, S.M. *J. Catal*. **2010**, *269*, 53.

[259] Tielens, F.; Calatayud, M.; Dzwigaj, S.; Che, M. *Microp. Mesop. Mater*. **2009**, *119*, 137.

[260] Tielens, F.; Dzwigaj, S. *Catal. Today* **2010**, *152*, 66–69.

[261] Tielens, F.; Dzwigaj, S. *Chem. Phys Lett*. **2010**, *501*, 59–63.

[262] Meeprasert, J.; Jungsuttiwong, S.; Namuangruk, S. *Microp. Mesop. Mat*. **2013**, *175*, 99.

[263] Zheng, A.; Han, B.; Li, B.; Liu, S.-B.; Deng, F. *Chem. Commun*. **2012**, *48*, 6936.

[264] Schoonheydt, R.A.; Geerlings, P.; Pidko, E.A.; van Santen, R.A. *J. Mater. Chem*. **2012**, *22*, 18705.

[265] Cook, S.J.; Chakraborty, A.K.; Bell, A.T.; Theodorou, D.N. *J. Phys. Chem*. **1993**, *97*, 6679.

[266] Teunissen, E.H.; van Duijneveldt, F.B.; van Santen, R.A. *J. Phys. Chem*. **1992**, *96*, 366.

[267] Brand, H.V.; Curtis, L.A.; Iton, L.E. *J. Phys. Chem*. **1992**, *96*, 7725.

[268] Kassab, E.; Fouquet, J.; Allavena, M.; Evleth, E.M. *J. Phys. Chem*. **1993**, *97*, 9034.

[269] Wang, X.; Lemos, M.A.N.D.A.; Lemos, F.; Ramôa Ribeiro, F. *Stud. Surf. Sci. Catal*. **2001**, *133*, 501.

[270] Haase, F.; Sauer, J. *J. Phys. Chem*. **1994**, *98*, 3083.

[271] Kassab, E.; Seiti, K.; Allavena, M. *J. Phys. Chem*. **1991**, *95*, 9425.

[272] Zygmunt, S.A.; Curtiss, L.A.; Iton, L.E.; Erhardt, M.K. *J. Phys. Chem*. **1996**, *100*, 6663.

[273] Zygmunt, S.A. *J. Phys. Chem. B* **2001**, *105*, 3034.

[274] Neyman, K.M.; Strodel, P.; Ruzankin, S.P.; Schlensog, N.; Knözinger, H.; Rösch, N. *Catal. Lett*. **1995**, *31*, 273.

[275] Khodakov, A.; Bates, S.P.; Dwyer, J.; Windsor, C.M.; Burton, N.A. *Phys. Chem. Chem. Phys*. **1999**, *1*, 507.

[276] Chandra, A.; Goursot, A.; Fajula, F. *J. Mol. Catal. A Chem*. **1997**, *119*, 45.

[277] Kyrlidis, A.; Cook, S.J.; Chakraborty, A.K.; Bell, A.T.; Theodorou, D.N. *J. Phys Chem*. **1995**, *99*, 1505.

[278] Greatbanks, S.P.; Sherwood, P.; Hillier, I.H.; Hall, R.J.; Burton, N.A.; Gould, I.R. *Chem. Phys. Lett*. **1995**, *234*, 367.

[279] Brändle, M.; Sauer, J. *J. Mol. Catal. A Chem*. **1997**, *119*, 19.

[280] Van der Mynsbrugge, J.; Hemelsoet, K.; Vandichel, M.; Waroquier, M.; Van Speybroeck, V. *J. Phys. Chem. C* **2012**, *116*, 5499.

[281] Grajciar, L.; Cejka, J.; Zukal, A.; Areán, C.O.; Palomino, G.T.; Nachtigall, P. *Chem. Sus. Chem.* **2012**, *5*, 2011.

[282] Yia, D.; Zhangb, H.; Deng, Z. *J. Mol. Catal. A Chem*. **2010**, *326*, 88.

[283] Liu, L.; Zhao, L.; Sun, H. *J. Phys. Chem. C* **2009**, *113*, 16051.

[284] Cheng, L.; Curtiss, L.A.; Assary, R.S.; Greeley, J.; Kerber, T.; Sauer, J. *J. Phys. Chem. C* **2011**, *115*, 21785.

[285] Datka, J.; Boczar, M.; Rymarowicz, P. *J. Catal*. **1988**, *114*, 368.

[286] Wojtaszek, A.; Ziolek, M.; Tielens, F. *J. Phys. Chem. C* **2012**, *116*, 2462.

[287] Elanany, M.; Su, B.-L.; Vercauteren, D.P. *J. Mol Catal. A Chem*. **2007**, *263*, 195.

[288] Solans-Monfort, X.; Sodupe, M.; Mó, O.; Yáñez, M.; Elguero, J. *J. Phys. Chem. B* **2005**, *109*, 19301.

[289] Sierka, M. Sauer, J. *J. Phys. Chem. B* **2001**, *105*, 1603.

[290] Oliveira, P.; Borges, P.; Ramos Pinto, R.; Lemos, M.A.N.D.A.; Lemos, F.; Védrine, J.C.; Ramôa Ribeiro, F. *Appl. Catal. A Gen*. **2010**, *384*, 177.

[291] Borges, P.; Ramos Pinto, R.; Oliveira, P.; Lemos, M.A.N.D.A.; Lemos, F.; Védrine, J.C.; Derouane, E.G.; Ramôa Ribeiro, F. *J. Mol. Catal. A Chem*. **2009**, *305*, 60.

[292] Borges, P.; Ramos Pinto, R.; Lemos, M.A.N.D.A.; Lemos, F.; Védrine, J.C.; Derouane, E.G; Ramôa Ribeiro, F. *J. Mol. Catal. A Chem*. **2005**, *229*, 127.

[293] Chu, Y.; Han, B.; Fang, H.; Zheng, A.; Deng, F. *Microp. Mesop. Mater*. **2012**, *151*, 241.

[294] Chu, Y.; Han, B.; Zheng, A.; Deng, F. *J. Phys. Chem. C* **2012**, *116*, 12687.

[295] Lesthaeghe, D.; Van Speybroeck, V.; Waroquier, M. *Phys. Chem. Chem. Phys*. **2009**, *11*, 5222.

[296] Rosenbach, Jr., N.; dos Santos, A.P.A.; Franco, M.; Mota, C.J.A. *Chem. Phys. Lett*. **2010**, *485*, 124.

[297] Boronat, M.; Concepción, P.; Corma, A.; Navarro, M.T.; Renz, M.; Valencia, S. *Phys. Chem. Chem. Phys*. **2009**, *11*, 2876.

[298] Esteves, P.M.; Louis, B. *J. Phys. Chem. B* **2006**, *110*, 16793.

[299] Pidko, E.A.; Mignon, P.; Geerlings, P.; Schoonheydt, R.A.; van Santen, R.A. *J. Phys. Chem. C* **2008**, *112*, 5510.

[300] Boronat, M.; Martínez-Sánchez, C.; Law, D.; Corma, A. *J. Amer. Chem. Soc*. **2008**, *130*, 16316.

[301] Boronat, M.; Martínez, C.; Corma, A. *Phys. Chem. Chem. Phys*. **2011**, *13*, 2603.

[302] Buurmans, I.L.C.; Pidko, E.A.; de Groot, J.M.; Stavitski, E.; van Santen, R.A.; Weckhuysen, B.M. *Phys. Chem. Chem. Phys*. **2010**, *12*, 7032.

[303] Bucko, T.; Benco, L.; Hafner, J.; Ángyán, J.G. *J. Catal*. **2011**, *279*, 220.

[304] Pidko, E.A.; van Santen, R.A. *J. Phys. Chem. C* **2007**, *111*, 2643.

[305] Li, G.; Pidko, E.A.; van Santen, R.A.; Feng, Z.; Li, C.; Hensen, E.J.M. *J. Catal*. **2011**, *284*, 194.

[306] Barone, G.; Armata, N.; Prestianni, A.; Rubino, T.; Duca, D.; Murzin, D, Yu. *J. Chem. Theory Comput*. **2009**, *5*, 1274.

[307] Nie, X.; Janik, M.J.; Guo, X.; Song, C. *Phys. Chem. Chem. Phys*. **2012**, *14*, 16644.

[308] Martin, A.; Checinski, M.P.; Richter, M. *Catal. Commun*. **2012**, *25*, 130.

[309] Papayannis, D.K.; Kosmas, A.M. *J. Mol. Struct. Theochem*. **2010**, *957*, 47.

[310] Hemelsoet, K.; Nollet, A.; Van Speybroeck, V.; Waroquier, M. *Chem. Eur. J*. **2011**, *17*, 9083.

[311] He, N.; Ding, Y.-h. *Microp. Mesop. Mater*. **2011**, *144*, 67.

[312] Svelle, S.; Tuma, C.; Rozanska, X.; Kerber, T.; Sauer, J. *J. Amer. Chem. Soc*. **2009**, *131*, 816.

[313] Van der Mynsbrugge, J.; Visur, M.; Olsbye, U.; Beato, P.; Bjørgen, M.; Van Speybroeck, V.; Svelle, S. *J. Catal*. **2012**, *292*, 201.

[314] Hammond, G.S. *J. Amer. Chem. Soc*. **1955**, *77*, 334.

[315] Zygmunt, S.; Curtiss, L.; Zapol, P.; Iton, L. *J. Phys. Chem*. **2000**, *104*, 1944.

[316] Guisnet, M.; Gnep, N.; Alario, F. *Appl. Catal*. **1992**, *89*, 1.

[317] Brenner, A.; Emmet, P. *J. Catal*. **1982**, *75*, 410.

[318] Krannila, H.; Haag, W.O.; Gates, B. *J. Catal*. **1992**, *135*, 115.

[319] Abbot, J. *Appl. Catal*. **1990**, *57*, 105.

[320] Lombardo, E.; Hall, W. *J. Catal*. **1988**, *112*, 565.

[321] Haw, J.; Richardson, B.; Oshiro, I.; Lazo, N.; Speed, J. *J. Amer. Chem. Soc*. **1989**, *111*, 2052.

[322] Haw, J.; Nicholas, J.; Xu, T.; Beck, L.; Ferguson, D. *Acc. Chem Res*. **1996**, *29*, 259.

[323] Kazansky, V.; Senchenya, I.; Frash, M.; van Santen, R. *Catal. Lett*. **1994**, *27*, 345.

[324] Kazansky, V.; Frash, M.; van Santen, R. *App. Catal. A Gen*. **1996**, *146*, 225.

[325] Blaszkowski, S.; Nascimento, M.; van Santen, R. *J. Catal*. **1996**, *100*, 3463.

[326] Rigby, A.; Kramer, G.; van Santen, R. *J. Catal*. **1997**, *170*, 1.

[327] Collins, J.; O'Malley, P. *Chem. Phys. Lett*. **1995**, *246*, 555.

[328] Kazansky, V.; Flash, M.; van Santen, R. *Catal. Lett*. **1997**, *48*, 61.

[329] Boronat, M.; Corma, A. *Appl. Catal. A Gen*. **2008**, *336*, 2.

[330] Fărcaşiu, D. *Catal. Lett*. **2001**, *71*, 95.

[331] Beyerlein, R.; McVicker, G.; Yacullo, L.; Ziemiak, J. *J. Phys. Chem*. **1988**, *92*, 1967.

[332] McVicker, G.; Kramer, G.; Ziemiak, J. *J. Catal*. **1983**, *83*, 286.

[333] McVicker, G.; Kramer, G.; Ziemiak, J. *J. Catal*. **1985**, *92*, 355.

[334] Mole, T.; Anderson, J.; Creer, G. *Appl. Catal*. **1985**, *17*, 141.

[335] Zygmunt, S.; Curtiss, L.; Zapol, P.; Iton, L. *J. Phys. Chem*. **2000**, *104*, 1944.

[336] Narbeshuber, T.; Vinek, H.; Lercher, J. *J. Catal*. **1995**, *157*, 388.

[337] Semenov, N.N. *Chemical Kinetics and Chain Reactions*, Oxford University Press, Oxford, **1935**.

[338] Horiuti, J.; Polanyi, M. *J. Mol. Catal. A Chem*. **2003**, *199*, 185.

[339] Evans, M.G.; Polanyi, M. *Trans Faraday Soc*. **1937**, *33*, 448.

[340] Evans, M.G.; Polanyi, M. *Trans. Faraday Soc*. **1936**, *32*, 1333.

[341] Masel, R.I. *Chemical Kinetics and Catalysis*, Wiley, New York, **2001**, 633.

[342] Marcus, R.A. *J. Phys. Chem*. **1968**, *72*, 891.

[343] Blowers, P.; Masel, R.I. *J. Phys*. *Chem. A* **1999**, *103*, 7047.

[344] Matsumoto, H.; Take, J.-I.; Yoneda, Y. *J. Catal*. **1970**, *19*, 113.

[345] Al-Khattaf, S.; Iliyas, A.; Al-Amer, A.; Inui, T. *J. Mol. Catal. A Chem*. **2005**, *225*, 117.

[346] Klyachko, A.L.; Kapustin, G.I.; Brueva, T.R.; Rubinstein, A.M. *Zeolites* **1987**, *7*, 119.

[347] Katada, N.; Kageyama, Y.; Takahara, K.; Kanai, T.; Begum, H.A.; Niwa, M. *J. Mol. Catal. A Chem*. **2004**, *211*, 119.

[348] Pinheiro, C.; Lemos, F.; Ribeiro, F. *Chem. Eng. Sci*. **1999**, *54*, 1735.

[349] Sun, L.; Guo, X.; Liu, M.; Wang, X. *Ind. Eng. Chem. Res*. **2010**, *49*, 506.

[350] Hashimoto, K.; Masuda, T.; Ueda, H.; Kitano, N. *Appl. Catal*. **1986**, *22*, 147.

[351] Martins, J.; Birot, E.; Guillon, E.; Lemos, F.; Ramôa Ribeiro, F.; Magnoux, P.; Laforge, S. *Microp. Mesop. Mater*. **2013**, *171* 230.

[352] Wang, X.; Lemos, M.A.N.D.A.; Lemos, F.; Ramôa Ribeiro, F. *Stud. Surf. Sci. Catal*. **2001**, *135*, 259.

[353] Fonseca, N.; Lemos, F.; Laforge, S.; Magnoux, P.; Ramôa Ribeiro, F. *React. Kinet. Mech. Catal*. **2010**, *100*, 249.

[354] Zheng, X.; Blowers, P. *J. Mol. Catal. A Chem*. **2005**, *229*, 77.

[355] Zheng, X.; Blowers, P. *J. Phys. Chem. A* **2005**, *109*, 10734.

[356] Ingelsten, H.H.; Zhao, D. Palmqvist, A.; Skoglundh, M. *J. Catal*. **2005**, *232*, 68.

[357] Katada, N.; Suzuki, K.; Noda, T.; Miyatani, W.; Taniguchi, F.; Niwa, M. *Appl. Catal. A Gen*. **2010**, *373*, 208.

[358] Niwa, M.; Noda, T.; Suzuki, K.; Morishita, N.; Katada, N. *Microp. Mesop. Mater*. **2011**, *146*, 208.

[359] Park, S.; Lee, J.; Song, J.H.; Kim, T.J.; Chung, Y.-M.; Oh, S.-H.; Song, I.K. *J. Mol. Catal. A Chem*. **2012**, *363–364*, 230.

[360] de O. Rodrigues, V.; Eon, J.-G.; Faro, Jr., A.C. *J. Phys. Chem. C* **2010**, *114*, 4557.

[361] Maihom, T.; Pantu, P.; Tachakritikul, C.; Probst, M.; Limtrakul, J. *J. Phys. Chem*. C **2010**, *114*, 7850.

[362] Lónyi, F.; Kovács, A.; Valyon, J. *J. Phys. Chem. B* **2006**, *110*, 1711.

[363] van Bokhoven, J.A.; Williams, B.A.; Ji, W.; Koningsberger, D.C.; Kung, H.H.; Miller, J.T. *J. Catal*. **2004**, *224*, 50.

[364] Ramachandran, C.E.; Williams, B.A.; van Bokhovenc, J.A.; Miller, J.T. *J. Catal*. **2005**, *233*, 100.

[365] Coelho, A.; Costa, L.; Marques, M.M.; Fonseca, I.; Lemos, M.A.; Lemos, F. *Reac. Kinet. Mech. Catal*. **2010**, *99*, 5.